

NASA TECHNICAL NOTE



NASA TN D-6700

c.1

NASA TN D-6700



LOAN COPY: RETURN
AFWL (DOUL)
KIRTLAND AFB, N M

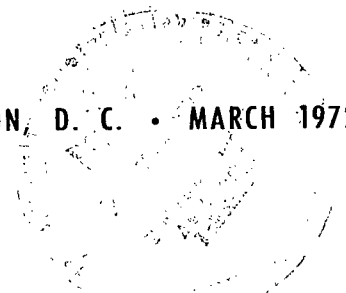
MONTE CARLO ANALYSIS OF LOBULAR
GAS-SURFACE SCATTERING IN TUBES
APPLIED TO THERMAL TRANSPIRATION

by Jerry D. Smith and Charles A. Raquet

Lewis Research Center

Cleveland, Ohio 44135

NATIONAL AERONAUTICS AND SPACE ADMINISTRATION • WASHINGTON, D. C. • MARCH 1972





0133430

1. Report No. NASA TN D-6700		2. Government Accession No.		3. Recipient's Catalog No.	
4. Title and Subtitle MONTE CARLO ANALYSIS OF LOBULAR GAS-SURFACE SCATTERING IN TUBES APPLIED TO THERMAL TRANSPIRATION				5. Report Date March 1972	
7. Author(s) Jerry D. Smith and Charles A. Raquet				6. Performing Organization Code	
9. Performing Organization Name and Address Lewis Research Center National Aeronautics and Space Administration Cleveland, Ohio 44135				8. Performing Organization Report No. E-6591	
12. Sponsoring Agency Name and Address National Aeronautics and Space Administration Washington, D. C. 20546				10. Work Unit No. 113-31	
15. Supplementary Notes				11. Contract or Grant No.	
16. Abstract A model of rarefied gas flow in tubes was developed, which combines a lobular distribution with diffuse reflection at the wall. The model with Monte Carlo techniques was used to explain previously observed deviations in the free molecular thermal transpiration ratio which suggest molecules can have a greater tube transmission probability in a hot-to-cold direction than in a cold-to-hot direction. The model yields correct magnitudes of transmission probability ratios for helium in Pyrex tubing (1.09 to 1.14), and some effects of wall-temperature distribution, tube surface roughness, tube dimensions, gas temperature, and gas molecular mass.				13. Type of Report and Period Covered Technical Note	
17. Key Words (Suggested by Author(s)) Lobular gas surface scattering; Gas-surface interaction; Thermal transpiration; Monte Carlo analysis; Tube transmission probabilities; Free molecular gas flow in tubes				14. Sponsoring Agency Code	
18. Distribution Statement Unclassified - unlimited					
19. Security Classif. (of this report) Unclassified		20. Security Classif. (of this page) Unclassified		21. No. of Pages 46	22. Price* \$3.00

MONTE CARLO ANALYSIS OF LOBULAR GAS-SURFACE SCATTERING IN TUBES APPLIED TO THERMAL TRANSPIRATION

by Jerry D. Smith and Charles A. Raquet

Lewis Research Center

SUMMARY

A model of free molecular gas flow in tubes has been developed which combines a temperature dependent lobular reflection distribution (Logan-Keck-Stickney) with diffuse reflection at the wall, using Monte Carlo calculation techniques. The model is used to explain previously observed deviations in the thermal transpiration ratio from the Knudsen limiting law. These deviations suggest that when two reservoirs at temperatures T_1 and T_2 are joined by a tube, gas molecules can be more likely to traverse the tube in the hot-to-cold direction than in the cold-to-hot direction; that is, $Q_{21} > Q_{12}$ when $T_2 > T_1$, where Q_{ij} is the tube transmission probability from reservoir i to reservoir j .

The model yields magnitudes of transmission probability ratios Q_{21}/Q_{12} for helium in Pyrex tubing in the range 1.09 to 1.14, consistent with some experimental thermal transpiration ratios with $T_1 = 77.4$ K, $T_2 = 295.0$ K. The model also yields some observed effects of wall-temperature distribution, tube surface roughness, tube dimensions, gas temperature, and gas molecular mass.

INTRODUCTION

It has generally been assumed that the pressures measured in two regions of a vacuum system in the free molecular range are related to their associated temperatures by the following relation, which will be referred to as the Knudsen limiting law (refs. 1 and 2)

$$R_m = \frac{P_1}{P_2} = \left(\frac{T_1}{T_2} \right)^{1/2} \quad (1)$$

However, several investigators (refs. 1 and 3 to 11) have noted deviations in the thermal transpiration ratio $R = P_1/P_2$ from this equation. (A list of symbols and their definitions is contained in the appendix.)

When the two regions are joined by a tube, this law (eq. (1)) results from the following argument: Assuming that gas entering the tube is Maxwellian, the requirement that

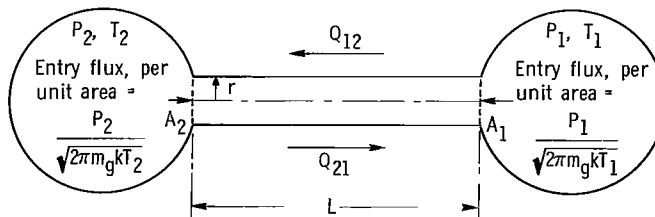


Figure 1. - Origin of conventional thermal transpiration ratio. Q_{ij} is the probability that a gas molecule in chamber i , which enters the connecting tube through plane A_i , will exit the tube through plane A_j ($i, j = 1, 2$).

the net mass flow through the tube be zero (see fig. 1) results in the following equation:

$$R = \frac{P_1}{P_2} = \left(\frac{Q_{21}}{Q_{12}} \right) \left(\frac{T_1}{T_2} \right)^{1/2} = a_T R_m \quad (2)$$

where Q_{ij} is the probability that a gas molecule in chamber i which enters the tube through plane A_i will exit the tube into chamber j through plane A_j . (See fig. 1.) The quantity $a_T = Q_{21}/Q_{12}$ is the ratio of tube transmission probabilities in the two axial directions. If $Q_{12} = Q_{21}$, then equation (2) yields equation (1).

It can be shown that the transmission probabilities Q_{12} and Q_{21} are equal if it is assumed, for example, that the gas-surface interaction at the tube wall is any one of simple temperature independent types such as the following (ref. 12):

- (1) Completely diffuse reflection (according to the cosine law)
- (2) Completely specular reflection
- (3) Some fixed degree of specular reflection regardless of the gas molecule's history; the molecule has a constant probability of being specularly reflected each time it strikes the wall; otherwise, it is diffusively reflected. This is Maxwell's interpretation of gas-surface interactions (ref. 13).

It has generally been assumed that for all gases, surfaces, and temperatures encountered in ordinary vacuum technology, the reflections are completely diffuse. Consequently, equation (1) has often been used for calculating the thermal transpiration ratio (TTR). However, some experiments (refs. 1 and 3 to 11) indicate that under certain conditions $a_T > 1.00$, implying that $Q_{21} > Q_{12}$, when $T_2 > T_1$. We will refer to the experimentally measured quantity $(P_1/P_2)/R_m = R/R_m$ as a_E , and the quantity Q_{21}/Q_{12} , which will be calculated theoretically in this report, as a_T . In particular, Hobson, Edmonds, and Verreault found, in the most extensive experimental studies of thermal transpiration to date, that a_E had values as large as approximately 1.31, for noble gases by Pyrex tubes, with $T_1 = 77.4$ K and $T_2 = 295.0$ K (refs. 8 to 11). In order to explain such behavior, one must assume a temperature-dependent reflection pattern at the smooth tube wall (different from the three temperature-independent reflection distributions described above), which results in a molecule having a greater probability of traversing the tube from the hot end to the cold end than in the opposite direction (ref. 9).

Edmonds and Hobson suggested that different degrees of specular reflection of hot and cold molecules could account for the directional difference in Q_{ij} (ref. 9). In line with this hypothesis, Miller and Buice (ref. 12) presented a temperature-dependent model for free molecular flow in a tube which explains the existence of the observed TTR deviations. Their model combined cosine law reflection (with complete temperature accommodation) with a degree of specular reflection (with no accommodation) dependent on the gas molecule energy. However, the transmission probabilities they calculated result in values of a_T ranging from approximately 1.33 to 2.18 for tubes of L/r (length/radius) varying from 2 to 50, respectively. In general, these theoretical values (a_T) were larger than experimental values (a_E), especially at higher L/r . Also, the trend of a_T increasing with increasing L/r , does not agree with data from Hobson and his co-workers (refs. 8 to 11), which indicate that a_E eventually levels off and probably decreases, not increases, with increasing L/r . It should be noted that the observed TTR deviations from the Knudsen law depend on parameters other than L/r , such as tube surface, the wall-temperature axial distribution, and the geometry of the reservoirs behind the tube entrance planes (planes A_1 and A_2 in fig. 1). These parameters were not extensively investigated by Miller and Buice.

In another approach, Hobson (refs. 11 and 14) has shown that a pipe with unequal conductances in two directions can validly describe an accommodation pump. Briefly, this pump multiplies the pumping rate of a single tube with differential transmission probabilities by using many such tube sections with their ends maintained at cold and hot temperatures. By analyzing observed pressure changes with time, he derived values of the two different conductances through the entire pump. The ratio of these directional conductances, agrees well with the ratio of equilibrium pressures at the ends of the

pump. But, Hobson does not consider in detail the microscopic origins of this difference in conductances (or, transmission probabilities) by dealing with the physical nature of the gas-surface interactions at the tube wall.

It is the purpose of this report to investigate possible origins of the observed inequality of transmission probabilities in single tubes with ends at different temperatures, using a gas-surface interaction model. A new model of rarefied gas flow in a cylindrical tube has been constructed. Gas molecule trajectories within the tube and transmission probabilities are calculated by Monte Carlo techniques. The basic difference between the approach presented herein and previous Monte Carlo studies is the following: Monte Carlo studies in the past have assumed complete diffuse reflection at the tube wall, or varying degrees of specular reflection (e.g., refs. 15 to 19). In the present model, each gas molecule approaching the surface is assigned a certain probability of undergoing a diffuse reflection. If not reflected diffusely, it is re-emitted in a direction chosen from a lobular distribution function, the shape and location of which (relative to the specular direction) is dependent on the gas and local surface temperatures. It will be shown that this temperature dependence results in the present model yielding a higher transmission probability in the hot-to-cold direction than the cold-to-hot direction.

PRACTICAL IMPORTANCE OF THERMAL TRANSPIRATION EFFECTS AND THE PRESENT MODEL

The importance of understanding TTR deviations from the Knudsen limiting law and their microscopic origins is twofold at the present time:

(1) The common use of the low pressure thermal transpiration effect is to deduce the pressure in one part of a vacuum system, perhaps inaccessible to a pressure gage, knowing the pressure in another part and the temperatures in the two parts. Such corrections are often made throughout the pressure range (free molecular to continuum) using analytic descriptions of the thermal transpiration ratio that contain the experimental low pressure limit R_m as a constant (e.g., Liang's formula, discussed in ref. 9). If this experimental low pressure limit is not the conventionally assumed low pressure limit of $R_m = (T_1/T_2)^{1/2}$, as is suggested in some experiments (refs. 1 and 3 to 11), then analytic descriptions using R_m yield incorrect values of the TTR at low (free molecular) pressures, as well as in the transition range.

(2) The pumping action of a tube with differential conductances caused by gas-surface interactions, termed accommodation pumping by Hobson, is a new pumping principle at low pressures (ref. 11). It could be of practical importance, particularly for pumping gases of low molecular weight.

The model in this report, utilizing the temperature dependent gas-surface reflection

distribution, presents another approach to the study of rarefied gases in tubes. Although the present study primarily deals with TTR effects, it may be also useful in interpreting other experiments involving gas-surface interactions.

Consider, for example, a tubulated pressure gage calibrated in a facility where one would not expect temperature-dependent gas-surface scattering to occur in the tube. Such a situation might occur with relatively cold gases and a cold, microscopically rough metallic tube surface. If this gage were used in a facility where lobular scattering in the tube could occur, even from conventional engineering surfaces (refs. 20 and 21), such as within or near the hot ($\gtrsim 1000$ or 2000 K) gas of a thruster plume, the calibration may no longer accurately correlate gage reading with gas pressure or density. The pressure reading may be deceptively high because more gas molecules are entering the gas ionization chamber than entered the chamber when the calibration was done, with strictly cosine reflection occurring.

In a related study, Ballance has considered various combinations of specular and diffuse reflections on the same molecular trajectory through a tube leading to the ionization region of a pressure gage (ref. 22). This was done in an effort to explain differences between neutral particle densities as determined from tubulated pressure gages and as determined from drag measurements on Explorer satellites containing the gages.

PRELIMINARY ANALYSIS AND THE MODEL

We will next describe in some detail the form of the lobular reflection pattern incorporated in the present tube model. The use of this equation is the principal new feature in the model. While this lobe equation has had considerable success in predicting observed reflection distributions of molecular beams scattered from flat surfaces, it is a fairly recent (1966) addition to gas-surface theory and is probably not familiar to all readers. After this discussion, the tube model will be described in detail, showing how typical molecule initial positions on the tube entrance planes and initial trajectories are generated by Monte Carlo techniques and how molecules are traced until they exit the tube, being reflected from the wall either diffusely or lobularly. The number of molecules successfully traversing the tube is divided by the number of initial trials, yielding calculated transmission probabilities.

Lobular Reflection Equation

The lobular reflection pattern used in our model is given by the equation predicted by the Logan, Keck, and Stickney (LKS) hard-cube model (refs. 23 and 24):

$$P(\theta_r) = \frac{3}{4} B_2 (1 + B_1 \sec \theta_i) \left(\frac{m_s T_g}{m_g T_s} \right)^{1/2} \left(1 + \frac{m_s T_g}{m_g T_s} B_1^2 \right)^{-5/2} \quad (3)$$

where

- $P(\theta_r)$ probability of reflection into $d\theta_r$ at θ_r
 T_g, T_s gas, surface temperatures, respectively
 μ m_g/m_s , ratio of masses of gas and surface atoms
 θ_i, θ_r angles of incidence and reflection measured from the surface normal, respectively

and where

$$B_1 = \left(\frac{1 + \mu}{2} \right) \sin \theta_i \cot \theta_r - \frac{(1 - \mu)}{2} \cos \theta_i$$

$$B_2 = \left(\frac{1 + \mu}{2} \right) \sin \theta_i \csc^2 \theta_r$$

This equation predicts the variation of reflected flux intensity as a function of angle of reflection after gas molecules have interacted with surface atoms simulated by independent smooth cubes oscillating with a Maxwellian energy distribution. An important assumption, experimentally confirmed for many gas-surface combinations (ref. 24), is that the tangential component of momentum of the gas molecule is unchanged during the interaction.

Concerning the use of the LKS equation in the present tube model, it is important to note the following: Strictly speaking, equation (3) is valid only when the gas molecules approaching the surface are characterized by a Maxwellian energy distribution, with some temperature T_g . In the present tube model, each gas molecule, including those reflected from the tube wall many times, is characterized by a temperature only, which is intermediate to the coldest and hottest wall temperatures. We do not deal explicitly with energy or velocity distributions, particularly of reflected molecules. To do so would greatly complicate the problem and is not necessary to explain several features of TTR deviations from the Knudsen limiting law. Stickney, Logan, Yamamoto, and Keck have shown that, based on the hard-cube model, little difference should be expected between the scattering of a thermal Maxwellian beam and an appropriate monoenergetic

beam (ref. 25). Smith, Saltsburg, and Palmer have verified this experimentally, for argon and xenon beams on silver surfaces (ref. 26). They state that the dispersion in scattered beams in typical thermal energy gas-surface studies results not so much from the velocity distribution in the incident beam or from surface roughness as from the dynamical nature of the surface atoms. The important experimental parameters are surface and gas temperatures.

It is important to note that we use the gas temperature to indicate average gas molecular kinetic energy. Hence, when we refer to hot gas or cold gas, we will mean gas molecules of high or low average kinetic energies, respectively. We do not deal explicitly with the spectrum of energies technically implied by a gas temperature. The relative lack of dependence of both observed and calculated reflected patterns on the velocity distribution in an incoming molecular beam partially supports our simplification of dealing strictly with temperatures. In the present model, we ascribe to each gas molecule the property of temperature, regarding temperature as a measure of average kinetic energy.

There are several reasons for the use of equation (3) in the present study of thermal transpiration effects:

(1) It contains explicit, experimentally verified dependences on gas molecular mass, surface molecular mass, angle of incidence, and gas and surface temperatures (see figs. 2 to 4). The experimental results are from Hinchey and Foley (ref. 27), and the calcu-

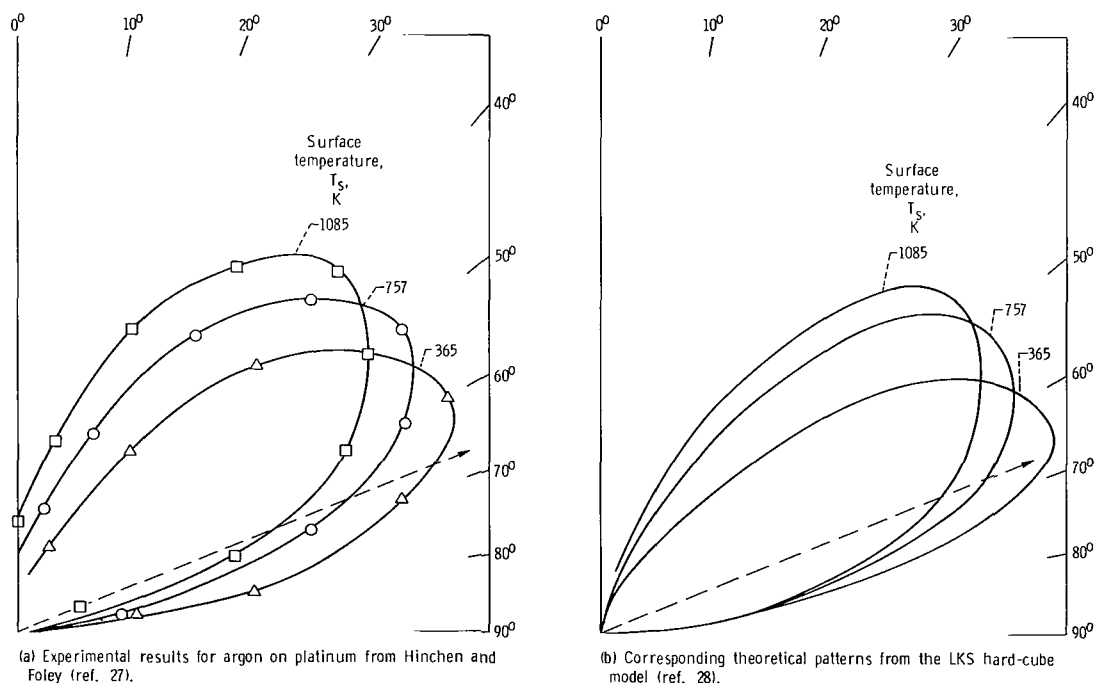
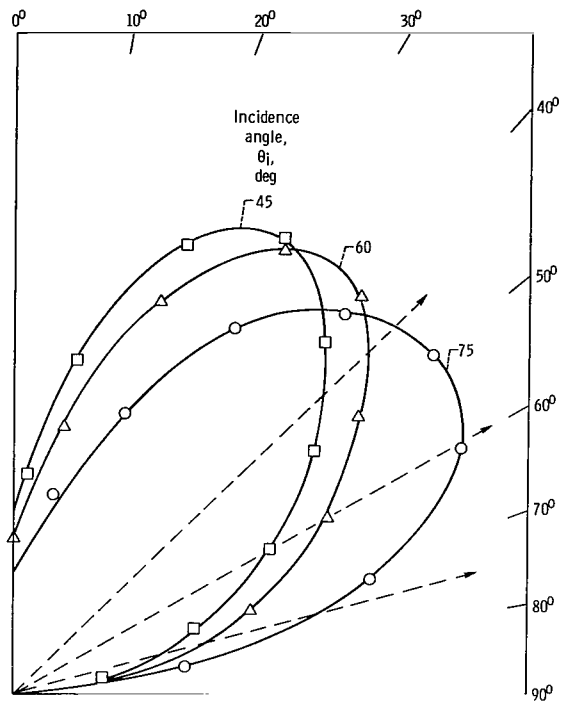
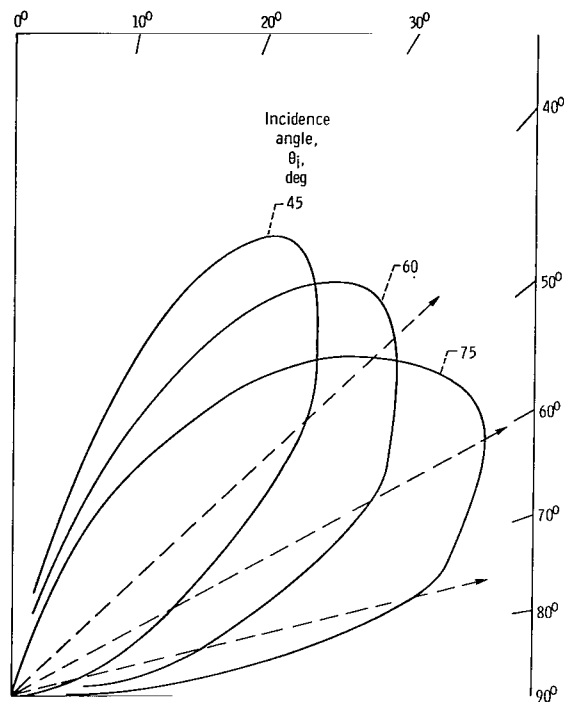


Figure 2. - Comparison of dependence of experimental and theoretical scattering distributions on surface temperature (from ref. 28). Argon on platinum; gas to surface atomic mass number ratio, 0.2; incidence angle, 67.5° ; gas temperature, 295 K.

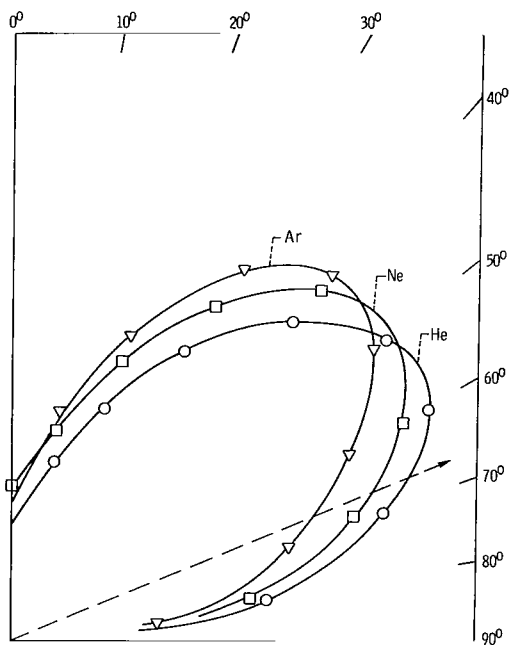


(a) Experimental results for argon on platinum from Hinchey and Foley (ref. 27).

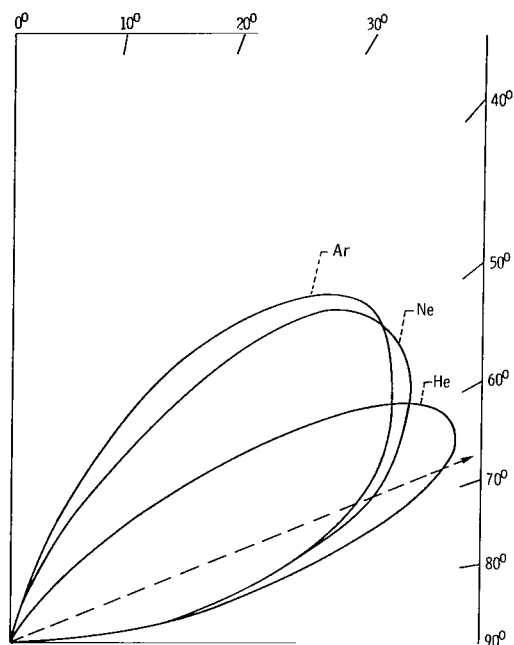


(b) Corresponding theoretical patterns based on the LKS hard-cube model (ref. 28).

Figure 3. - Comparison of dependence of experimental and theoretical scattering distributions on the angle of incidence (from ref. 28). Argon on platinum; gas to surface atomic mass number ratio, 0.2; gas temperature, 295 K; surface temperature, 1081 K.



(a) Experimental results for helium, neon, and argon on platinum (ref. 27).



(b) Corresponding theoretical results from the LKS hard-cube model (ref. 28).

Figure 4. - Comparison of dependence of experimental and theoretical scattering distributions on mass of incident gas atoms (from ref. 28). Platinum surface; gas to surface atomic mass number ratio, 0.02 for helium, 0.10 for neon, and 0.20 for argon; incidence angle, 67.5° ; gas temperature, 295 K; surface temperature, 1073 K.

lated patterns are from simple hard-cube theory (ref. 28). These dependencies result in theoretical explanations of several aspects of TTR deviations. It should be noted that the theoretical distributions in these figures result from an earlier version of the hard-cube theory (nonclosed form, ref. 28), not from the use of equation (3). However, the scattering patterns given by this equation agree closely with those given by the analysis in reference 28 (ref. 23).

Of particular importance in the present study are the recent experimental observations of O'Keefe and Palmer of nondiffuse scattering of a 300 K helium beam from 300 K polished glass (ref. 29). For example, for $\theta_i = 70^\circ$, they observed a rather broad reflection lobe with a maximum in the range $\theta_r = 40^\circ$ to 60° . For comparison, a lobe maximum at about 62° is predicted by the LKS equation (eq. (3)), using $\mu = 0.21$ (to approximate the helium-on-glass mass ratio), $\theta_i = 70^\circ$, and $T_R = T_s/T_g = 1.00$. (Their observed patterns also showed substantial reflected intensity at $\theta_r < 0^\circ$; i.e., some molecules were backscattered, which is consistent with the assumption in the present model that some molecules are reflected according to the cosine law.) For argon on smooth glass, O'Keefe and Palmer noticed that the same nondiffuse trends, but to a much lesser degree. In general, for argon they corroborated results of Hurlbut (ref. 30), who observed predominantly diffuse scattering.

(2) The LKS equation is probably the simplest closed-form reflection pattern other than diffuse reflection, which has experimental confirmation. This relative simplicity is quite important in terms of computer time because Monte Carlo simulation of many gas trajectories in very long tubes can be quite time consuming.

(3) In general, cube models, which may seem grossly oversimplified to those familiar with the nature of real surfaces, have had considerable success in the treatment of gas-surface interactions. The hard-cube model, valid only for single gas-surface atom collisions and for the gas-to-surface mass ratios μ less than $1/3$, yields good scattering distribution agreement for lighter mass gas species. A modification of this model by Logan and Keck involving the addition of a potential well (the soft-cube model, ref. 31) gives better scattering distribution agreement with heavier gas molecules ($\mu > 1/3$) and accounts for multiple collisions. However, the soft-cube equations are probably too complicated to use in Monte Carlo calculations. It might also be noted that the soft-cube model has been used to successfully predict energy accommodation coefficients for rare gases on tungsten (ref. 32). Also, Goodman has recently described a quantum mechanical basis for the cube models (ref. 33).

The Model

The Monte Carlo approach to rarefied gas dynamics problems involves the generation of many typical molecular trajectories according to certain assumed probability

distributions, and then appropriate averaging of the properties of the individual molecules resulting from those trajectories and the various gas-gas (if any) or gas-surface interactions sustained. With gas-surface scattering dependent on temperatures and incident angles, whether an incoming gas molecule eventually exits the tube out the far end depends in a complicated way on its trajectory history. The calculation of transmission probabilities in the present problem is more amenable to a Monte Carlo technique than to integral equation solutions of the Clausing type.

The basic idea in the present model of allowing molecules to be reflected at the tube wall either diffusely or lobularly is similar to Maxwell's useful intuitive concept of combining cosine and specular reflection (ref. 13). Trilling (ref. 34) has suggested combining cosine and hard-cube lobular patterns to describe some complicated observed patterns, arguing that a fraction of incoming molecules strike "hard-cube positions" on the surface while the remainder undergo multiple collisions either with a single surface layer atom or with microscopic roughness asperities and are hence re-emitted diffusely. Observed reflected distributions of molecular beams scattered from a small area of surface (such as the patterns for helium on polished glass, ref. 29) sometimes resemble superpositions of diffuse and lobular patterns.

The calculation proceeds in a manner similar to other Monte Carlo treatments of gases in tubes. The basic theorem is the following (e.g., ref. 35, p. 314): If a random variable ξ has the normalized probability density function $f(u)$, $u_0 \leq u \leq u_1$, then the probability density function of a random variable η , defined as

$$\eta = \int_{u_0}^{\xi} f(u) du \quad (4)$$

is uniform in the interval $(0, 1)$. Hence, if we wish to obtain a number belonging to a set of random numbers $\{S_i\}$, which has the known or assumed density function $f(u)$, we merely solve the following equation for the upper limit S_i :

$$\int_{u_0}^{S_i} f(u) du = R_i \quad (5)$$

where R_i is a random variable with a uniform probability density function on $(0, 1)$. (As in other Monte Carlo treatments, values for R_i are provided by a computer sub-program in our calculations.)

We assume that the initial position of the gas molecule is uniformly distributed on the entrance plane of the tube and that the probability of being emitted in a particular direction from a surface (or, plane) is directly proportional to the cosine of the angle

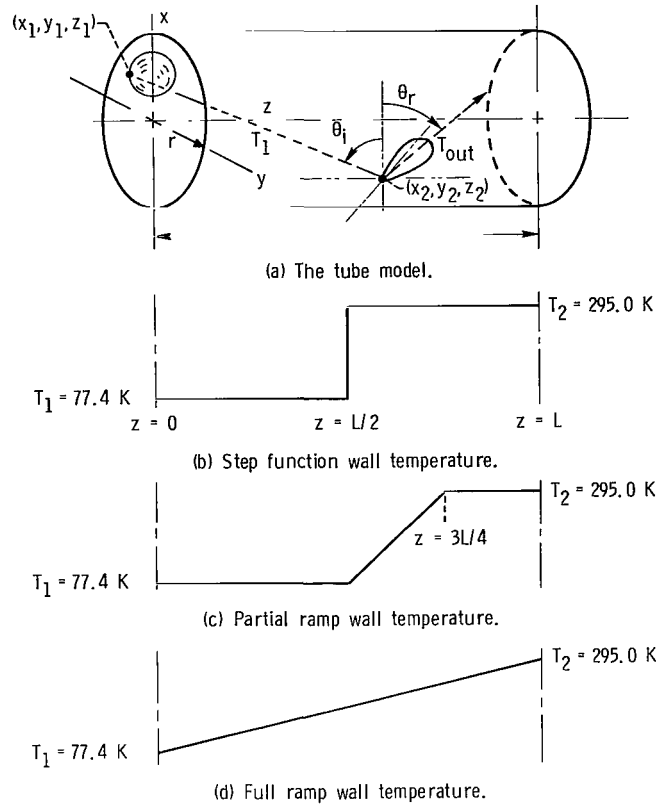


Figure 5. - Present tube model showing lobular reflection at the wall and three assumed wall temperature distributions.

between that direction and the surface normal. Using appropriate forms for $f(u)$ in equation (5) (uniform and cosine law probability density functions), it can be shown that one proper choice of initial coordinates and direction cosines (see fig. 5) is the following:

$$x_1 = r \sqrt{R_1} \cos(2\pi R_2) \quad (6a)$$

$$y_1 = r \sqrt{R_1} \sin(2\pi R_2) \quad (6b)$$

$$z_1 = 0 \quad (6c)$$

$$\cos(A_1) = \sqrt{R_3} \cos(2\pi R_4) \quad (6d)$$

$$\cos(B_1) = \sqrt{R_3} \sin(2\pi R_4) \quad (6e)$$

$$\cos(C_1) = \sqrt{1 - R_3} \quad (6f)$$

With this initial position and direction, the intersection (x_2, y_2, z_2) of the trajectory with the cylinder of radius r is calculated. If $z_2 > L$, then the molecule has exited the tube with no wall hits, and is counted both toward the direct tube transmission probability Q_D , the probability that a molecule passes through the tube with no wall hits, and the total tube transmission probability Q_{ij} , the probability that a molecule eventually leaves the tube through the exit plane, regardless of the number of wall collisions. If $0 \leq z_2 \leq L$, then the simulated molecule has struck the tube wall, and decisions are then made as to whether the particle will be trapped permanently, or re-emitted diffusely or with the LKS lobe distribution, and what the re-emission temperature will be. For the present study, we have used a trapping probability of 0.0, since appreciable adsorption or surface diffusion is unlikely for the gases, temperatures, and tube sizes of present concern (ref. 11).

A constant probability of a diffuse reflection F_C was assumed. The probability of a lobular reflection is then $F_L = 1 - F_C$. In this respect, the present model differs from that of Miller and Buice (ref. 12) and from the suggestion of Edmonds and Hobson (ref. 9) concerning hotter molecules having a greater probability of being specularly reflected than cold molecules.

Following the gas-wall hit, the choice of a diffuse or lobular reflection is made by first choosing another random number, say R_5 . If $R_5 \leq F_C$, we choose the reflection to be diffuse, determining the new direction cosines in the local coordinate system on the wall (with (x_2, y_2, z_2) as origin; see fig. 5) according to equations (6d) to (6f), only with newly chosen random numbers. Then, the intersection of this new trajectory with the cylinder is calculated. If $R_5 > F_C$, then the re-emission will be lobular, and the calculation of direction cosines is more complicated.

The LKS probability distribution $P(\theta_r)$, equation (3) is a two-dimensional reflection pattern, in a plane formed by the incident trajectory and the surface normal at the point of impact. (See fig. 5.) To choose a reflection direction θ_r , $0 \leq \theta_r \leq \pi/2$, measured from the surface normal in the appropriate plane according to $P(\theta_r)$, the approach using equation (5) is not used. Although $P(\theta_r)$ can be integrated in closed form, the integration does not lead to a simple solution for the upper limit in equation (5). Instead of a numerical solution for this limit, the following procedure was used (based on, e.g., ref. 35, p. 319): $P(\theta_r)$ was normalized by its calculated maximum value $P(\theta_{\max})$, yielding $P_N(\theta_r)$; $0 \leq P_N(\theta_r) = P(\theta_r)/P(\theta_{\max}) \leq 1$. Next, a pair of random numbers

was chosen, R_i, R_{i+1} . Letting $\theta_r = (\pi/2)R_i$, we compare $P_N(\theta_r)$ with R_{i+1} . If $R_{i+1} < P_N(\theta_r)$, we accept the direction θ_r . The other two direction cosines in the local wall coordinate system follow from the known θ_i and the chosen θ_r , and the next cylinder intersection can be calculated. If $R_{i+1} \geq P_N(\theta_r)$, we reject the pair R_i, R_{i+1} , choose a new pair of random numbers, and repeat the process. We continue the process until we find an $R_{i+1} < P_N(\theta_r)$, or until 10 such attempts have been made at which time we abandon further choosing and merely send the molecule off at θ_{\max} , its most probable value. It can be shown that such a procedure will statistically result in a choice of θ_r in accordance with the probability distribution function $P(\theta_r)$. It can be looked upon as "throwing a dart" at a unit square and accepting the coordinates so chosen only if the point lies below the curve $P_N(\theta_r)$ (ref. 35, p. 319).

When the molecule is reflected from the tube wall, its temperature is changed to T_{OUT} , according to the following formulas using Knudsen's familiar concept of the temperature accommodation coefficient (ref. 36):

$$T_{\text{OUT}} = \alpha_C \left[T_s(z) - T_{\text{IN}} \right] + T_{\text{IN}}, \quad \text{for cosine reflection} \quad (7)$$

$$T_{\text{OUT}} = \alpha_L \left[T_s(z) - T_{\text{IN}} \right] + T_{\text{IN}}, \quad \text{for lobular reflection} \quad (8)$$

where α_C and α_L are constant temperature accommodation coefficients for cosine and lobular reflections, respectively, and $T_s(z)$ is an assumed wall-temperature distribution, like those shown in figures 5(b) and (c). For the initial gas-wall collision, T_{IN} will be either T_1 or T_2 , depending on whether we are tracing molecules from the cold-to-hot and/or hot-to-cold end, respectively. Note that T_{OUT} for one gas-wall interaction will become T_{IN} for the next interaction, if there is one.

After each new intersection is calculated, a test is made to see whether the molecule has left the tube through the entrance plane ($z = 0$), or out the exit plane ($z = L$), or has struck the tube wall again. If the molecule has left the tube, another initial molecular trajectory is generated according to equations (6a) to (6f), and the procedure is repeated.

The entire process is repeated until a specified number of trials K_0 (typically 10 000), have been completed. All trials are first performed for molecules entering the tube from the cold reservoir T_1 . Then, the entire process is repeated for K_0 additional trials, for molecular entry from the hot reservoir T_2 , with appropriate changes in initial gas temperature and $T_s(z)$.

The total number of molecules initially at T_i which eventually leave the tube through the exit plane is divided by K_0 , yielding a calculated value of Q_{ij} . The total number of molecules leaving the tube directly from the entrance plane through the exit plane is divided by K_0 , yielding the quantity Q_D . This direct transmission probability

Q_D , not of particular interest in the present TTR studies, is independent of axial direction because molecules directly transmitted never encounter the wall and, hence, never experience temperature-dependent reflection. (Therefore, Q_D results were used only as a check on the calculations and will not be presented.) The theoretical value of the TTR, normalized by the temperature factor $(T_1/T_2)^{1/2}$, is given by

$$a_T = \frac{Q_{21}}{Q_{12}} \quad (9)$$

Also calculated are the following: (1) the average number of gas-wall collisions per incoming gas molecule initially at T_i , $K_{GW}(k, j)$, which will be seen to also indicate the existence of TTR deviations from the Knudsen limiting law, (2) the axial distribution of these collisions, expressed as wall flux, (3) the axial distribution of average gas temperatures of molecules striking the wall, and (4) the average temperatures of molecules leaving the tube through the two end planes.

It should be noted that the calculated average temperatures are only simple averages: total temperature divided by total numbers of particles. Temperature, like any gas transport property, should properly be calculated using velocity weighting procedures. However, gas velocity magnitude changes at the surface and resultant reflected velocity distributions were not dealt with specifically in the present model. We have simplified the energy exchange by using temperature accommodation coefficients, as discussed in the next section.

Use of Temperature Accommodation Coefficients

The use of equations (7) and (8) involves a major simplification and departure from the LKS theory: simple, constant temperature accommodation coefficients dictating the reflected molecules' temperatures (or, energies). The LKS theory predicts a certain velocity distribution at any given reflected angle θ_r , and, from this distribution, a most probable velocity at any angle θ_r (ref. 23). However, the LKS hard-cube velocity predictions have not as yet had the success experimentally that the directional predictions, such as those shown in figures 2 to 4, have had. Some experimental determinations of average reflected molecule energies (i. e., temperatures) indicate a variation of average reflected gas temperature with θ_r , with some trends different from LKS predictions (refs. 21, 37, and 38). Other reflected gas temperatures have been measured to be fairly independent of θ_r (e. g., refs. 20 and 21). To the authors' knowledge, no reflected gas energy distributions have been measured for light mass gases (such as helium) on glass surfaces. Only a few measurements of accommodation coefficients for light

mass gases on glass have been made (ref. 39). For most of the present work, we used the value $\alpha = 0.35$, from reference 39.

It should be mentioned that at present it is not unusual for a gas-surface interaction model to predict only certain gas-surface properties successfully. It is generally known that the cube models predict scattering patterns well and that some lattice theories (in which incoming gas atoms interact with a one-, two-, or three-dimensional lattice of atoms in the solid) successfully predict thermal accommodation coefficients (ref. 40). The interaction assumed in the present tube model can be regarded as a reasonable and convenient hybrid. We incorporate the LKS scattering direction predictions with the more conventional simpler ideas of cosine reflection and temperature change through accommodation coefficients, to yield a tractible Monte Carlo problem. Although the present model is convenient, it should be noted that it is not really self-consistent: the use of a temperature accommodation coefficient is inconsistent with the assumption in the LKS model that the tangential component of momentum is unchanged during the interaction. However, even if the LKS velocity distributions were verified, we feel that sampling from both directional and velocity magnitude distributions would require prohibitive computer time for the present study. Fortunately, our calculated values of Q_{ij} are relatively insensitive to α_C and α_L , which could indicate that values of long tube transmission probabilities (hence, of a_T) are not very sensitive to gas temperature (or, energy) changes at each gas-surface interaction.

Statistical Accuracy of Transmission Probabilities

As a measure of the statistical accuracy of Q_{ij} , the 95-percent confidence interval or limit for Q_{ij} is calculated

$$\epsilon_N = 1.96 \sqrt{\frac{Q_{ij}(1 - Q_{ij})}{K_o}} \quad (10a)$$

This interval is interpreted as follows: Monte Carlo calculations of Q_{ij} based on K_o trials should be within ϵ_N of the exact theoretical answer 95 percent of the times the calculation is done, assuming that the answers are normally distributed about the theoretical answer. This is usually a reasonable assumption if Q_{ij} is not extremely small. The theoretical value of Q_{ij} should be used in equation (10a), but since its value for the present problem is unknown, the calculated value will be used. The most general estimate of Monte Carlo error (when no assumptions are made about the distribution of calculated Q_{ij} 's) is given by the Chebyshev inequality

$$|Q_{ij}(\text{Monte Carlo}) - Q_{ij}(\text{theoretical})| \leq \sqrt{\frac{Q_{ij}(\text{theoretical})[1 - Q_{ij}(\text{theoretical})]}{pK_o}} = \epsilon_C \quad (10b)$$

where p is the probability of falsity of the inequality in equation (10b). (From ref. 35, p. 12.) The quantity $(1 - p) \times 100$ percent is referred to as confidence, and the quantities ϵ_N and ϵ_C are confidence limits or intervals. For 95-percent confidence ($p = 0.05$),

$$\epsilon_C = 4.47 \sqrt{\frac{Q_{ij}(\text{theoretical})[1 - Q_{ij}(\text{theoretical})]}{K_o}} \quad (10c)$$

Our use of $\epsilon_N (< \epsilon_C)$ is to some extent justified by comparison of our results for transmission probabilities with previous analytical results, for 100-percent diffuse reflection and for partial specular reflection at the tube wall. This will be discussed in the first part of the RESULTS AND DISCUSSION section, which follows. The important feature of all estimates of Monte Carlo error is the inverse dependence on the square root of the number of trials. Quadrupling the number of trials only halves the confidence interval.

RESULTS AND DISCUSSION

In the following sections, we first compare results of the present calculation of transmission probabilities with some previous theoretical results, where applicable, to show the accuracy of the present model. Then a brief summary of some previous thermal transpiration ratio (TTR) experiments is given, listing the specific parametric effects which a theoretical tube model must attempt to explain. Next, preliminary to the results of the generation of molecular trajectories in the tube model, some properties of LKS lobular reflections are discussed, with emphasis on gas and surface temperature dependence. Then, we present results for tube transmission probabilities and results concerning numbers of gas-wall collisions, when both cosine law and lobular reflections occur at the tube wall. Finally, we show to what extent the model is capable of explaining the various experimental TTR effects observed.

Comparison with Previous Theoretical Tube Transmission Probability Results

The results of the present model can be compared with previous studies for which all reflections from the wall are diffuse by setting $F_C = 1.0$. Our tube transmission probabilities in table I, presented as functions of L/r , are within ϵ_N of all but one of other analytical and Monte Carlo results shown (refs. 41 to 45), particularly those of

TABLE I. - TUBE TRANSMISSION PROBABILITIES FOR COMPLETELY DIFFUSE (COSINE LAW)
REFLECTIONS AT THE WALL ($F_C = 1.0$, IN THE PRESENT MODEL)

Tube length to radius ratio, L/r	Number of Monte Carlo trials, K_0	Tube trans- mission probability ^a (present model), Q_{ij}	95-percent confidence interval, ϵ_N	Previous values of Q_{ij}				
				Richley and Reynolds (ref. 41)	DeMarcus (ref. 42)	Clausing (ref. 43)	Ward and Fraser (Monte Carlo, with K_0 400 000) (ref. 44)	Miller (ref. 45)
0.5	40 000	0.801275	0.0039	0.801	0.80127	0.8013	-----	0.80128
1.0	10 000	.6772	.0092	.671	.67198	.6720	0.6724	.67209
2.0	10 000	.5102	.0098	.513	.51423	.5136	-----	.51472
4.0	10 000	.3580	.0094	.355	.35658	.3589	.3570	.35629
10.0	20 000	.19025	.0054	-----	.19099	.1973	.1914	.18656

^a $Q_{12} = Q_{21} = Q_{ij}$ independent of direction when $F_C = 1.0$.

TABLE II. - TUBE TRANSMISSION PROBABILITIES FOR
PARTIAL SPECULAR REFLECTION AT THE WALL

[Tube length to radius ratio, 2.0; number of Monte
Carlo trials, 20 000; probability of specular
reflection, $1.0 - F_C$.]

Probability of cosine law reflection, F_C	Tube transmission probability, ^a Q_{ij}		95-percent confidence interval, ϵ_N
	DeMarcus (ref. 47)	Present model	
1.0	0.51423	0.51625	0.0069
.8	.58247	.58235	.0068
.6	.65890	.6588	.0066
.4	.74693	.7476	.0060
.2	.85412	.8535	.0049
0	1.00000	1.0000	0

^a $Q_{12} = Q_{21} = Q_{ij}$, independent of direction.

DeMarcus, which are regarded as probably the most accurate (refs. 44 and 46). (The exception is Clausing's value for $L/r = 10.0$. But Clausing's values for higher L/r are believed now to be relatively inaccurate (ref. 44).)

We can also essentially duplicate DeMarcus' results for partial specular reflection (ref. 47) by replacing the procedure of choosing θ_r from $P(\theta_r)$ when a lobular reflection is chosen, with the simple specular condition $\theta_r = \theta_i$. Our results for $L/r = 2.0$ are shown in table II as a function of F_C and are again within ϵ_N of DeMarcus' answers.

Another comparison with previous theory concerns the use of an assumed constant nonzero trapping probability (or, sticking coefficient) at each gas-tube wall collision. Smith and Lewin (ref. 17) calculated tube transmission probabilities as a function of L/r and the sticking coefficient at the wall, using cosine law reflection for particles not trapped at the wall. The present model essentially reproduces these results also. (However, as mentioned previously, for the present TTR studies, a sticking coefficient of zero was used.)

Summary of Some Previous Experiments

There are many factors that could affect TTR deviations. Several of these factors

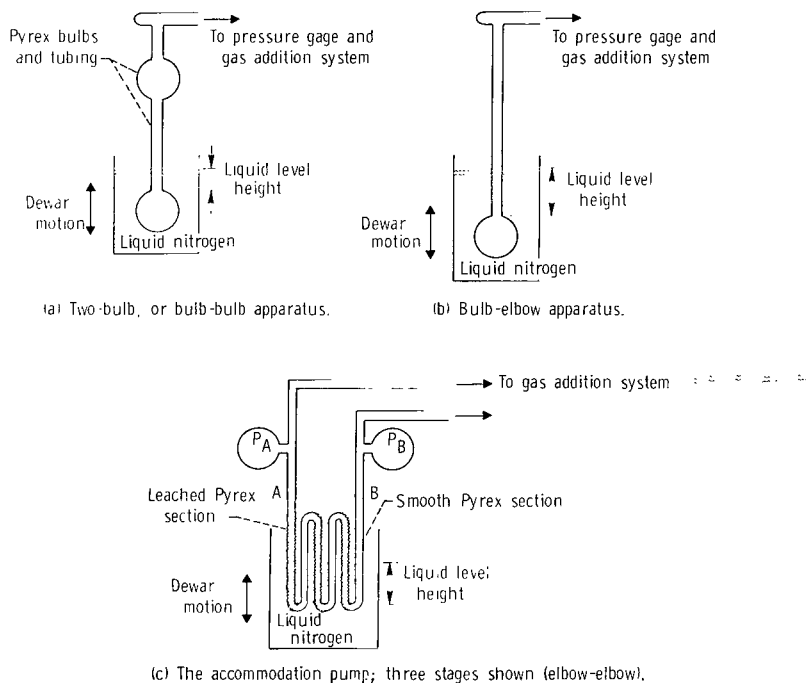


Figure 6. - Schematics of types of apparatus used to investigate the thermal transpiration ratio by Hobson's group (refs. 8 to 11)

have been determined experimentally, particularly in the extensive studies of Hobson's group (refs. 8 to 11 and 14). In the following brief summary of the effects suggested by these experiments, the TTR effects will be discussed in terms of the quantity $a_E = R/R_m$, which will be referred to as the temperature normalized thermal transpiration ratio (experimental).

Effect of reservoir geometry. - Figure 6 shows the three types of apparatus used by Hobson's group to investigate the thermal transpiration ratio. These types are characterized by the "volumes" joined by the tubes being either glass bulbs, or 90 or 180° elbows. In general, the lower part of each apparatus was dipped into liquid nitrogen to varying levels, probably giving rise to a fairly sharp wall-temperature break in the tubes. The pressure in the cold region (P_1) was derived from the pressure in the hot region (P_2) and some other measurable parameters assuming conservation of gas phase molecules (ref. 9). Generally, values of a_E in the elbow apparatus (figs. 6(b) and (c)) are larger than and more sensitive to liquid nitrogen level variations than a_E values in the two-bulb apparatus (fig. 6(a)) (ref. 9). For example, for helium with the liquid nitrogen level half way up the tube, elbow apparatus values range approximately from 1.13 to 1.31, while two-bulb apparatus values are roughly 1.03 to 1.11.

Effect of wall-temperature distribution. - As stated before, for elbow apparatus, a_E was sensitive to liquid-nitrogen level, increasing with increasing nitrogen height and then either leveling off as the height increased or going through a maximum (fig. 7 and ref. 9). Note that, in general, a_E is still not equal to 1.00 even when the entire tube is at a single temperature, particularly when the tube is at 295.0 K (liquid-nitrogen height at 0 cm in fig. 7). For the two-bulb apparatus data, a_E is more insensitive to the liquid-nitrogen level (fig. 7 and ref. 9). The addition of a heater wrapped around the tube right above the liquid-nitrogen level, which probably sharpened the wall-temperature break, either slightly lowered the value of R (or, a_E) or left it unchanged (fig. 7, sample 1, with and without heater).

Effect of gas type. - All other factors held constant, for the noble gases, a_E decreases with increasing gas mass. For a tube with $L/r \approx 13.6$, a_E varied from about 1.18 ± 0.01 for helium ($m_g = 4$) to about 1.05 ± 0.01 for xenon ($m_g = 130$) (ref. 11).

Effect of tube material. - The results of Hobson (ref. 11) as well as those of Lund and Berman (ref. 48), suggest that metal tubulation, no matter how smooth or rough the surface may be, results in values for a_E within a few percent of the expected value 1.00; tube transmission probabilities do not appear to be directionally dependent. So, the larger TTR deviations from Knudsen's limiting law seem at present to be restricted to smooth Pyrex tubulation.

Effect of surface preparation. - Hobson found that leaching the Pyrex tubes (i. e., microscopically roughening their surfaces by the action of HCl) caused the TTR deviations to virtually vanish. The greater the degree of leaching, the closer the TTR ap-

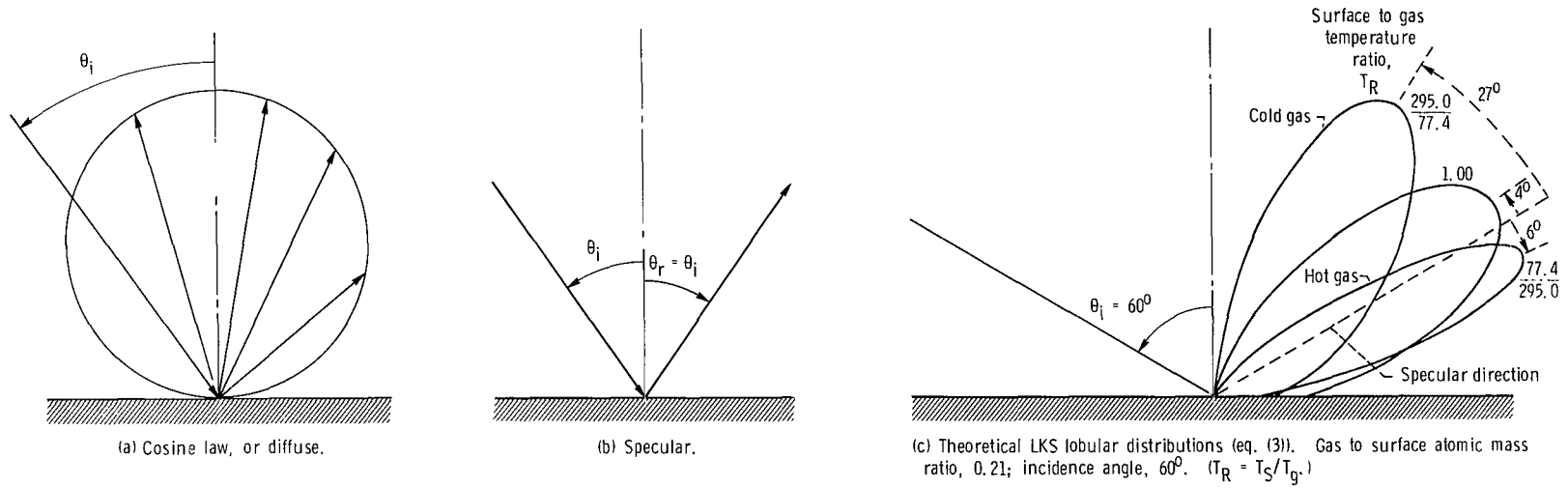


Figure 8. - Three types of gas-surface reflection patterns.

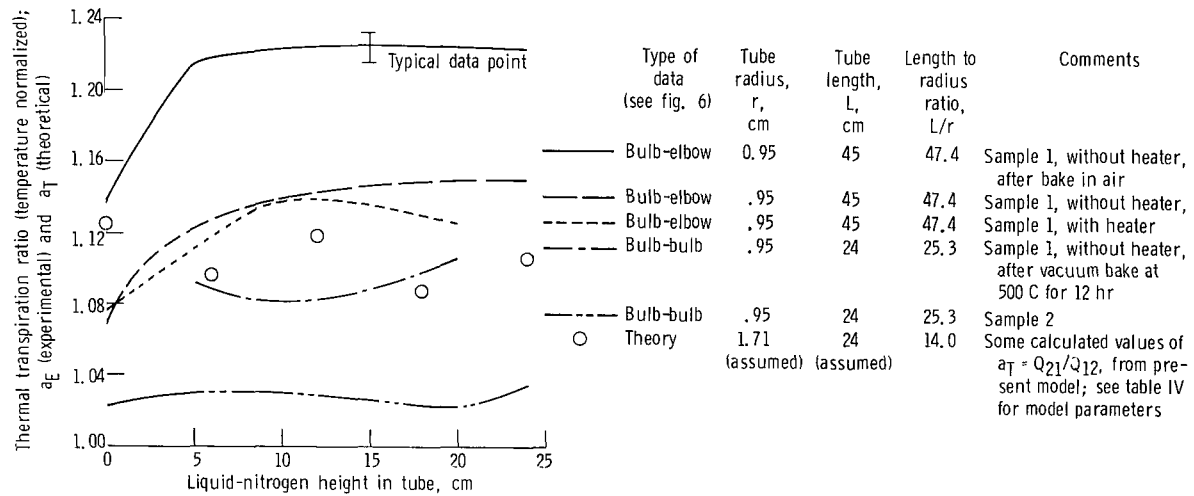


Figure 7. - Normalized thermal transpiration ratio for helium as function of liquid-nitrogen height in tube. Data for curves from Edmonds and Hobson (ref. 9); $T_1 = 77.4$ K; $T_2 = 295.0$ K; $P_2 \approx 4 \times 10^{-6}$ torr.

proached the anticipated theoretical value R_m (ref. 10).

Effect of preadsorbed gas layers. - When layers of Ar, Kr, or Xe were preadsorbed on the Pyrex tube, the value of a_E for helium was unchanged (ref. 11).

Effect of tube L/r . - This effect, although not clearly established, seems to indicate that the Knudsen limiting law (eq. (1)) holds for apertures ($L/r = 0.0$) and that, beyond a certain L/r , a_E decreases with increasing L/r , perhaps back to 1.00. The existence of a maximum (or of maxima) is hence suggested at some intermediate L/r .

Effect of number of stages in a multistage pump. - Using the finding that leaching removes the directional difference in tube conductance, Hobson combined leached tubes with smooth tubes in the arrangement shown in figure 6(c), each leached-smooth tube combination forming a stage. The effect of increasing the number of stages was to increase the pumping action of a single smooth tube with the ends at different temperatures. For helium the value of the pump ratio P_A/P_B in the three-stage pump was 2.10; in the 28-stage pump, 23.3. For a single-stage pump, the ratio, which is then theoretically equivalent to the previously defined a_E (ref. 11), was 1.18 ± 0.01 .

Effect of hot chamber temperature T_2 . - The warm half of a three-stage pump was changed from 295 to 600 K, resulting in an increase in pump ratio for helium from 2.10 to 2.50. Although this increase cannot be reliably extrapolated to a single-stage pump or just one smooth tube (ref. 11), the qualitative trend of a_E increasing with the hot-gas - hot-tube temperature was established.

Lobular Reflection Distributions

Shown in figure 8 are various types of possible reflection patterns: cosine law, specular, and lobular. In such diagrams as figures 8(a) and (c), the probability of emission in a certain direction is proportional to the length of the radius vector in that direction, as shown in figure 8(a). The LKS distributions (fig. 8(c)) depend on temperature only through the ratio $T_R = T_s/T_g$ and on the nature of the gas and surface only through the mass ratio $\mu = m_g/m_s$. In figure 8(c) and throughout the paper, the value of $\mu = 0.21$ was used for helium on Pyrex (sodium borosilicate), after estimating the average mass of an atom in the glass surface at $m_s = 19.2$ by weighting the masses of species within the Pyrex in proportion to their occurrence in the bulk. Considering the complicated structure of glass, μ must be regarded to a certain extent as an adjustable parameter. However, our results for $a_T = Q_{21}/Q_{12}$ are not extremely sensitive to this parameter.

It should be noted that the exceptionally good agreement between theoretical and experimental reflection distributions in figures 2 to 4 occurs, coincidentally, in a situation where the mass ratio $\mu \cong 0.2$ (argon on platinum). Since the LKS model depends on the

ratio of masses, it does not matter theoretically whether the ratio $\mu \cong 0.2$ arises from argon on platinum, or from helium on Pyrex with an assumed $m_s = 19.2$.

Because the experimental arrangements being considered should result in a fairly sharp wall-temperature break, one would expect many collisions in the tube with $T_R = T_s/T_g = 77.4/295.0$ (hot gas on a cold wall) and with $T_R = 295.0/77.4$ (cold gas on a hot wall). Figure 8(c) shows that the lobe for the hot gas on a cold wall is directed away from the specular direction toward the surface tangent and the lobe for the cold gas on a hot wall is directed more toward the surface normal. It is this differential displacement of lobular patterns, on either side of the specular direction, that results in the difference in tube transmission probabilities suggested by $a_E > 1.0$. One would also expect gas-wall collisions in the tube with $T_R = 1.0 = 77.4/77.4 = 295.0/295.0$, where the gas and wall temperatures are the same. However, there is no differential in lobe position for a hot gas on a hot wall and a cold gas on a cold wall, because the temperature ratio is 1.0 in either case.

Figure 9 shows the difference between the calculated angular position of lobular maximum θ_{max} and the specular direction $\theta_{spec} = \theta_i$ as a function of θ_i for the three values of T_R mentioned previously. It is seen that the differential displacement is always present for $\theta_i > 0^\circ$ and that the effect increases as the angle of incidence increases. In particular, for the cold gas on a hot wall ($T_R = 295.0/77.4$) the lobes are displaced strongly toward the surface normal for large angles of incidence (large negative values of $\Delta\theta$ in fig. 9). For $T_R = 1.0$, the lobe maximums are also displaced above the specular direction, the effect increasing with increasing θ_i , but to a much lesser extent than lobes with $T_R = 295.0/77.4$.

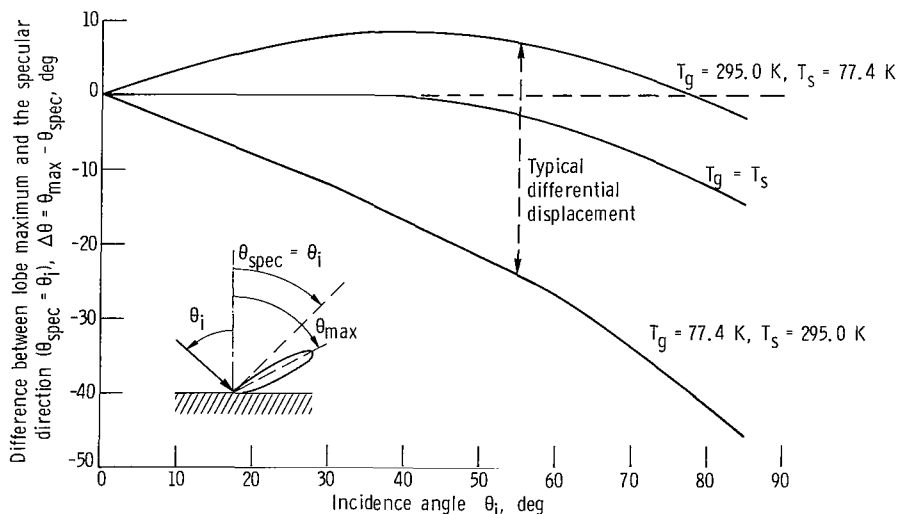


Figure 9. - Difference between lobe maximum and specular direction ($\Delta\theta = \theta_{max} - \theta_{spec}$ where $\theta_{spec} = \theta_i$) as function of incidence angle (from eq. (3)). Gas to surface atomic mass number ratio, 0.21.

These properties of lobular reflections will be used in interpreting results for partial lobular reflection in tubes.

Partial Lobular Reflection in Tubes - Transmission Probabilities and Gas-Wall Collisions

The parameter F_C , the probability of a gas molecule collision with the wall being followed by a diffuse reflection, must be regarded as an adjustable parameter, considering what is now known about gas-surface interactions. Figure 10 shows the effect of varying F_C on the two transmission probabilities Q_{12} and Q_{21} . For these calculations, $L/r = 14.0$, which is typical of some tubes used by Hobson, Edmonds, and Verreault (refs. 8 and 11); $\mu = 0.21$, as discussed previously, $K_o = 10\ 000$, which, by equation (10a), leads to the 95-percent confidence limits shown; $\alpha_C = \alpha_L = 0.35$, an experimental value for helium on glass measured between about 250 and 400 K and relatively temperature independent in that range (ref. 39); and $T_s(z)$ is the step function shown in figure 5(b). Also, we have assumed that F_C is the same constant for all gas-wall collisions, independent of gas or surface temperatures or angles of incidence. Note

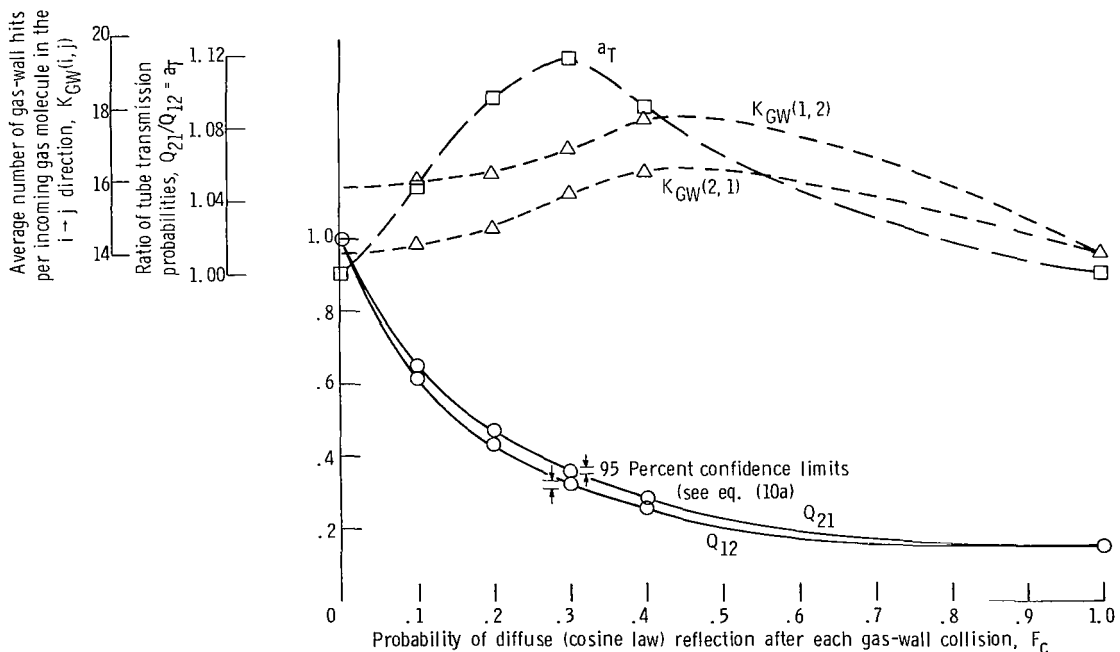


Figure 10. - Dependences of transmission probabilities, the ratio of transmission probabilities, and the average number of gas-wall collisions per incoming molecule on the probability of cosine reflection at wall. Tube length to radius ratio, 14.0; number of Monte Carlo trials, 10 000; temperature accommodation coefficient, $\alpha = \alpha_C = \alpha_L = 0.35$; gas to surface atomic mass number ratio, 0.21; step function wall temperature distribution (see fig. 5(b)).

in figure 10 that, when $F_C = 0.0$ and all reflections are lobular, $Q_{12} = Q_{21} = 1.000$, as expected, since with no backscattering possible all molecules must traverse the tube starting from either end. Note also that when $F_C = 1.0$ and all reflections are diffuse, $Q_{12} \cong Q_{21} \cong 0.147$, since no temperature-dependent scattering has then occurred. Between these two values of F_C we find $Q_{21} > Q_{12}$ and $a_T > 1.00$, which is consistent with the experimentally observed TTR effect, that is, $a_E > 1.00$.

The maximum value of a_T in figure 10 is $a_T = 1.119$ when $F_C \cong 0.3$. In the range $0.1 < F_C < 0.6$, values of a_T are in the approximate range $1.05 < a_T < 1.119$, which is consistent with values from some two-bulb data (fig. 7), but somewhat less than the magnitudes of a_E from elbow data. We might expect our theoretical results to compare better with two-bulb data because molecular entry from a large bulb into the tube would be expected more Maxwellian, as assumed in our model, than entry through an elbow into the tube.

As shown in figure 10, $K_{GW}(1,2)$ the average number of gas-wall collisions per incoming molecule in the $T_1 - T_2$ direction, is greater than $K_{GW}(2,1)$. Thus, initially hot molecules T_2 make slightly fewer wall collisions, on the average, than the initially cold molecules T_1 starting at the opposite tube end. Through the remainder of this report, the subscript 2 will refer to the hot temperature (gas or wall), and the subscript 1 will refer to the cold temperature. We have extrapolated with dashed lines in figure 10 the curves for $K_{GW}(i,j)$ to their calculated common value of about 14.0 at $F_C = 1.0$ and to their approximate expected values at $F_C = 0.0$. Note that when $F_C = 0.0$, even though all molecules ultimately transverse the tube starting from either reservoir, we would not expect the average number of gas-wall collisions in the cold-to-hot direction $K_{GW}(1,2)$ to equal $K_{GW}(2,1)$. The reason for this is the differential displacement of typical lobular patterns in the two different axial directions caused by different typical wall-to-gas temperature ratios in those directions. The $K_{GW}(i,j)$ curves go through a maximum and decrease to a common value of 14.0, as F_C goes to 1.0. As the probability of diffuse reflection increases, more molecules are backscattered out the entrance plane soon after they enter the tube and hence make fewer total gas-wall collisions.

Figure 11 shows how the wall flux varies axially, when $F_C = 0.3$ and $L/r = 14.0$. The wall-temperature break between 77.4 and 295 K is located at $L/2$. The tube was divided into 35 equal axial segments. For 10 000 initial trials from the entrance plane, simulating an inlet flux of molecules entering from the 77.4 K reservoir, the total number gas-wall hits in each segment was divided by the surface area of the segment, yielding a local wall flux. This wall flux was then divided by the inlet flux. The procedure was repeated with 10 000 trials at the other tube end, with molecules initially at 295.0 K. Note that the wall flux for incoming 77.4 K molecules beyond the tube center $L/2$ (where the temperature break occurs), going generally in the direction $T_1 \rightarrow T_2$, is greater

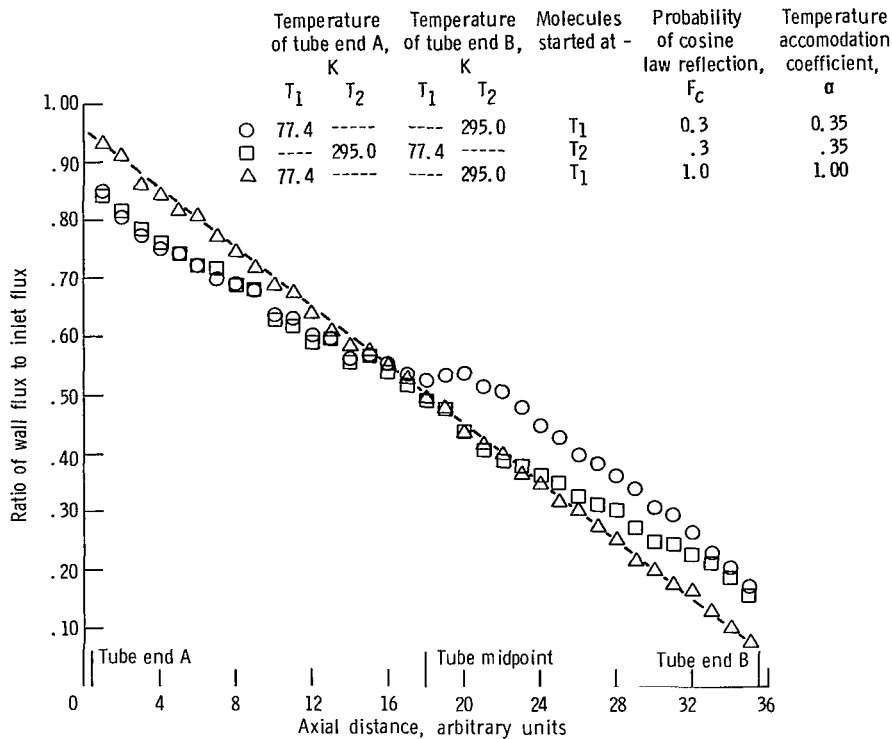


Figure 11. - Variation of wall flux (normalized by flux entering tube) with axial position in tube. Tube length to radius ratio, 14.0; number of Monte Carlo trials, 10 000; gas to surface atomic mass number ratio, 0.21; step function wall temperature distribution with temperature change at midpoint.

than the wall flux for incoming 295.0 K molecules beyond the tube center, going generally in the opposite direction, $T_2 \rightarrow T_1$. Thus, the difference in the average collision numbers $K_{GW}(1, 2)$ and $K_{GW}(2, 1)$ arises from gas-wall collisions after the molecules cross the wall-temperature break, which was placed near the center of the tube to approximate experimental conditions.

Figure 11 also shows that the wall flux is very nearly linear in the axial coordinate when $F_C = 1.0$ and all gas-wall reflections are diffuse. This well-known result was originally an assumption in Clausing's integral equation approach to tube transmission probabilities and has been verified by many analytical studies since then (e.g., refs. 15 and 41). Also, the normalized flux at the midpoint of the tube when $F_C = 1.0$ is very nearly 0.5, which also agrees with previous studies (e.g., ref. 41).

Note in figure 11 that the two wall flux distributions when F_C is only 0.3 are still fairly linear. Lobular reflections (forward scattering processes) tend to send incoming molecules down the tube more so than diffuse reflections, which results in smaller impact densities near the tube entrance plane (the left tube end in fig. 11) when $F_C = 0.3$.

Comments on Statistical Accuracy

Throughout this study, because of the length of computer time required for calculations involving lobular reflections in long tubes, a compromise had to be made between the number of cases studied and the accuracies of transmission probabilities for a given set of parameters. The 95-percent confidence intervals for Q_{ij} are in the range $\epsilon_N = 0.007$ to 0.0096 when $K_O = 10\,000$ and are always small enough to statistically insure that $Q_{21} > Q_{12}$. As mentioned before, to halve the ϵ_N , we must quadruple the number of Monte Carlo trials K_O or equivalently, quadruple the computer time. Doubling the number of trials to $K_O = 20\,000$ had little effect on answers in typical situations, as seen by comparing cases 1 and 2 in table III.

TABLE III. - EFFECTS OF PARAMETRIC VARIATIONS IN PRESENT MONTE CARLO TUBE MODEL

[Probability of cosine law reflection, 0.3; step function wall temperature (see fig. 5(b)) unless otherwise noted.]

Case	Gas-to-surface atomic mass ratio, μ	Tube end temperature, K		Tube length to radius ratio, L/r	Number of Monte Carlo trials at each tube end, K_O	Temperature accommodation coefficient, α	Tube transmission probability		Transmission probability ratio, $a_T = Q_{21}/Q_{12}$	Average number of gas-wall hits per incoming gas molecule	
		T_1	T_2				Q_{12}	Q_{21}		$K_{GW(1,2)}$	$K_{GW(2,1)}$
1	0.21	77.4	295.0	14.0	10 000	0.35	0.3229	0.3614	1.119	17.0	15.9
2	↓	↓	↓	↓	20 000	↓	.3244	.3623	1.117	16.9	15.9
a ₃	↓	↓	↓	↓	10 000	↓	.2931	.3637	1.241	19.1	16.7
b ₄	↓	↓	↓	↓	↓	↓	.3332	.3707	1.113	16.8	16.1
c ₅	↓	↓	↓	↓	↓	↓	.3217	.3625	1.127	16.8	16.0
6	↓	↓	↓	↓	↓	1.00	.3224	.3664	1.137	16.9	16.2
7	↓	↓	↓	↓	↓	$\left\{ \begin{array}{l} \alpha_C = 1.00 \\ \alpha_L = 0.35 \end{array} \right\}$.3309	.3648	1.102	17.1	15.8
8	.33	↓	↓	↓	↓	.35	.3340	.3630	1.087	16.5	15.2
9	.21	↓	↓	6.0	↓	↓	.5335	.5390	1.010	7.5	6.8
10	.21	↓	↓	20.0	15 000	↓	.2617	.2910	1.112	24.0	22.2
11	.21	↓	600.0	14.0	10 000	↓	.3130	.3638	1.162	17.2	15.7

^aAll lobular reflections at θ_{max} only.

^bPartial ramp function (fig. 5(c)).

^cFull ramp function (fig. 5(d)).

A trial case was investigated in which each lobularly reflected molecule was assigned a reflection angle corresponding to the direction of the lobe pattern maximum θ_{max} . For $L/r = 14.0$, $F_C = 0.3$, $\alpha = 0.35$, and $\mu = 0.21$, we found $a_T = 1.241$ when all lobular emissions were at θ_{max} only. This number is different from $a_T = 1.119$, which resulted when sampling from the LKS distribution was done (see cases 1 and 3 in table III). Hence, although the computer time was less by about a third, the shorter

procedure of sending all lobularly reflected molecules off in the direction of the lobe maximum was not proper. Molecules reflected above and below θ_{\max} apparently play an important role in determining the magnitude of a_T . Therefore, the more time consuming process of sampling from the LKS distribution must be done.

Dependence on Wall-Temperature Distribution

The transmission probabilities Q_{12} and Q_{21} depend on the axial position of the step function wall-temperature break in the model as shown in table IV and figure 12. Both Q_{12} and Q_{21} increase as the proportion of the tube that is cold increases, with Q_{21} being always larger than Q_{12} . As the liquid level increases, a smaller part of the tube is hot. Hence, we would expect fewer cold gas - hot wall collisions. These kind

TABLE IV. - DEPENDENCE OF TUBE TRANSMISSION
PROBABILITIES ON POSITION OF WALL-
TEMPERATURE DISCONTINUITY (STEP
FUNCTION) CALCULATED BY USE
OF PRESENT MODEL)

[Tube length to radius ratio, 14.0; number of Monte Carlo trials, 10 000; temperature accommodation coefficient, 0.35; gas-to-surface atomic mass ratio, 0.21; probability of cosine law reflection, 0.3; $T_1 = 77.4$ K, $T_2 = 295.0$ K.]

Position of wall-temperature discontinuity, from tube end T_1	Tube transmission probability		Transmission probability ratio, $a_T = Q_{21}/Q_{12}$
	Q_{12}	Q_{21}	
a_0	0.3008	0.3384	1.125
$\frac{L}{4}$.3138	.3441	1.097
$\frac{L}{2}$.3229	.3614	1.119
$\frac{3L}{4}$.3378	.3677	1.089
b_L	.3384	.3745	1.107

^aEntire tube at $T_2 = 295.0$ K.

^bEntire tube at $T_1 = 77.4$ K.

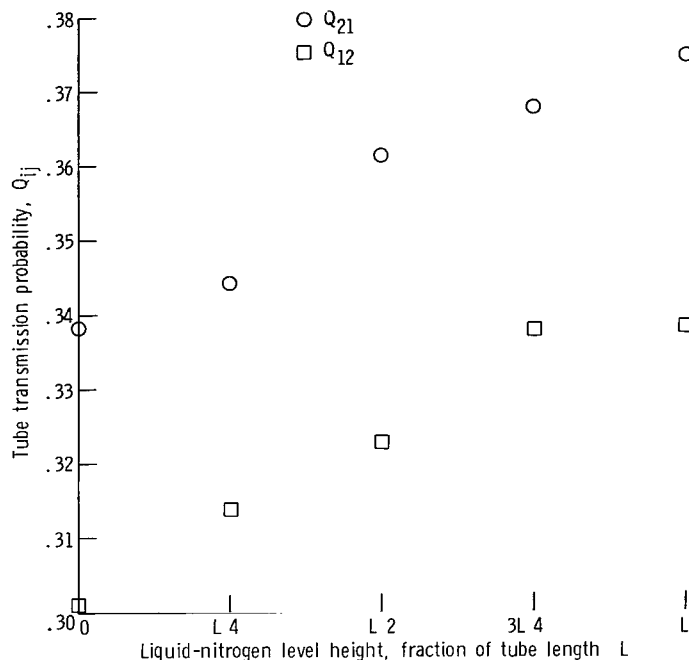


Figure 12. - Variation of Q_{12} and Q_{21} with liquid-nitrogen level height using the present model. Tube length to radius ratio, 14.0; number of Monte Carlo trials, 10 000; temperature accommodation coefficient, 0.35; gas to surface atomic mass number ratio, 0.21; probability of cosine law reflection, 0.3. A step function, between $T_1 = 77.4$ K and $T_2 = 295.0$ K, is used to simulate the nitrogen level.

of collisions, considering lobular reflections, work to hinder cold gas motion toward the hot end. Therefore, Q_{12} increases. We would also expect more hot gas - cold wall collisions as the level rises, for gas entering the hot tube end, which works to aid hot-gas motion toward the cold end. Hence, Q_{21} also increases. However, both values increase in such a way that $a_T = Q_{21}/Q_{12}$ remains relatively unchanged. This is consistent with observed two-bulb behavior.

A comparison of these values of a_T (fig. 12) with some experimental values a_E is shown in figure 7. The theoretical values (for $L/r = 14.0$) are in the range of experimental values for the two-bulb data with $L/r = 25.3$. A detailed quantitative comparison is not intended: calculations with $L/r = 25.3$ would require much more computer time. (However, additional results indicate changing L/r from 14.0 to 20.0 affects a_T only slightly.) The difference between supposedly similar tubing samples 1 and 2 in figure 7 points up the facts that knowledge of the nature of glass surfaces is incomplete and that reproducibility of glass surfaces could be difficult to achieve experimentally. One could explain such a difference by assuming a larger F_C for sample 2, which might be expected if the inner surface of sample 2 was microscopically rougher than that of sample 1.

Both experimental results and the results of the model calculations indicate that even when the liquid-nitrogen level is at $z = 0$ or $z = L$ and the entire tube is assumed to be at 295.0 or 77.4 K, respectively, values of a_E (or a_T) can still be greater than one. From the standpoint of thermal transpiration ratios, this implies that there can be a difference between two chambers joined by an aperture (which leads to $a_E = 1.00$) and two chambers joined by a tube at the temperature of one of the chambers. In the model, even if the tube is at a single temperature, say, 295.0 K, that portion of the incoming 77.4 K gas that is reflected lobularly can experience cold gas - hot wall reflections, which hinders passage through the tube. The 295.0 K gas entering from the other end can only have lobular reflections with $T_R = 295.0/295.0 = 1.00$.

Another indication of the insensitivity of a_T to the tube wall-temperature distribution between the 77.4 and 295.0 K chambers is the following: Instead of a step function for $T_S(z)$, as shown in figure 5(b), which led to $a_T = 1.119$ (case 1, table III), we used the partial ramp function in figure 5(c). This led to $a_T = 1.113$ (case 4, table III). The use of a full ramp function, with $T_S(z)$ linear between $z = 0$ and L , led to $a_T = 1.127$ (case 5, table III). One might expect the step function to approximate the wall-temperature distribution with a heater wrapped around the tube just above the liquid-nitrogen level; and the partial ramp (or full ramp) function might better approximate the wall-temperature distribution without the heater. Although Edmonds and Hobson did not present heater - no heater results from two-bulb apparatus, they found in their elbow experiments that the heater either lowered the value of a_E or left it unchanged. Our results indicate almost no change.

Considering the calculated magnitudes of a_T and the insensitivity of a_T to temperature variations along the tube, the present model appears to simulate two-bulb data better than elbow data.

Effects Involving the Nature of the Gas

Hobson, Edmonds, and Verreault did most of their studies with elbow apparatus rather than two-bulb apparatus, since they were interested in obtaining and investigating the larger deviations from $a_E = 1.00$. Bearing in mind the possibility of effects due to nonMaxwellian tube entry conditions, we will next consider several parameters which were experimentally investigated only in non-two-bulb apparatus. Unless otherwise stated, the subsequent calculations will be with $F_C = 0.3$, $L/r = 14.0$, $\mu = 0.21$, $K_O = 10\ 000$, and the step function wall-temperature distribution in figure 5(b). The value $F_C = 0.3$ was chosen since it yielded a_T values comparable with those obtained experimentally (fig. 7).

Varying the species of the gas molecules can be considered in the model in three

ways: varying α_C and/or α_L , the temperature accommodation coefficients; varying $\mu = m_g/m_s$; and varying F_C , the probability of a diffuse reflection. As mentioned previously, experimental results indicate that, as the mass of noble gases increases, measured values of a_E more closely approach 1.00. It has also been observed (e.g., ref. 49) that thermal accommodation coefficients of gases on most surfaces generally increase as the gas mass increases. The effect of mass changes through accommodation coefficient changes was investigated by calculating Q_{12} , Q_{21} , and a_T with $\alpha_C = \alpha_L \equiv \alpha = 1.00$ (retaining $\mu = 0.21$) and comparing with previous answers using $\alpha_C = \alpha_L \equiv \alpha = 0.35$. When $\alpha = 0.35$, we find $a_T = 1.119$, and, if $\alpha = 1.00$, then $a_T = 1.137$. (See cases 1 and 6, table III.) Increasing α to 1.00 has little effect on Q_{12} , Q_{21} , or a_T . Other accommodation coefficient changes also result in relatively small changes in a_T . For example, if $\alpha_C = 1.00$ and $\alpha_L = 0.35$, then $a_T = 1.102$ (case 7, table III). Thus, varying the two temperature accommodation coefficients for diffusely and lobularly reflected molecules between 0.35 (an experimental value for helium on glass) and 1.00 (the commonly assumed value for most gases on most surfaces) results in, at most, a 2- to 3-percent change in a_T .

To examine the effect of the mass ratio within the LKS distribution, values of Q_{12} , Q_{21} , and a_T were calculated for $\mu = 0.33$ and 0.21. Changing μ from 0.21 to 0.33 changed a_T from 1.119 to 1.087, a slight change in the correct experimental direction. (See cases 1 and 8, table III.) It was impossible to use a larger mass ratio appropriate for neon, for example. Using the assumption about the typical mass of a glass surface atom, the ratio would then be $(20.18/19.2) \cong 1.05$. The LKS theory is valid only for $\mu < 1/3$, hence the limiting value $\mu = 0.33$ was used.

There is another mass effect which is probably more important than the direct effect of μ in the LKS distribution in explaining (within the model) why a_E decreases as m_g increases. It is plausible to expect that the probability of a diffuse reflection F_C increases with increasing m_g . The more diffuse gas-surface reflections there are (i.e., the larger F_C is) the less effect differential lobular scattering has on tube transmission probabilities. The scattering patterns observed by O'Keefe and Palmer (ref. 29) show that argon is reflected from polished glass surfaces much more diffusely than is helium. Generally, the larger the gas molecular mass, the more efficient is the energy transfer in a gas-surface interaction and the more likely a multiple collision or temporary adsorption is, which is usually thought to be followed by diffuse re-emission. However, current knowledge of gas-surface interactions is not complete enough to allow a reliable correlation of F_C with gas mass. Varying F_C in such a way as to obtain a specific observed mass trend in the thermal transportation ratios would be of doubtful value without some theoretical foundation.

Effects Involving the Nature of the Surface

Surface parameters also affect TTR values. A quantitative explanation for surface effects requires a more sophisticated tube model. Specifically, what is probably needed is a detailed correlation of F_C with gas and surface properties. When tubes are smooth, polished metal, Lund and Berman (ref. 48) found that transmission probabilities are fairly accurately predicted by theory and are not very temperature dependent. Consistent with this finding, Hobson (ref. 11) found for metal tubes that normalized ratios a_E in TTR experiments varied from unity by no more than several percent. Attempting to simulate such situations within the LKS distribution, preliminary calculations (meaning, with low values of K_O , the number of Monte Carlo trials) were done using a mass ratio $\mu = 0.07$, appropriate for helium on iron, nickel, or stainless steel. These preliminary calculations indicate as much or more difference in Q_{12} and Q_{21} when $\mu = 0.07$ as when $\mu = 0.21$. However, it is not certain whether the LKS model adequately predicts scattering patterns for μ values much below about 0.10. Theoretical lobes for $\mu = 0.02$ (helium on platinum) are considerably thinner (narrower) than corresponding experimental lobes (fig. 4).

It is likely that metal tubes, like increased gas molecular mass, lead to increased probabilities of diffuse reflection. This result might be expected by virtue of a deepened interaction potential between gas and surface molecules, or as a result of reflections within microscopic surface asperities. An increase in F_C is also the obvious explanation for Hobson's observations that in leached Pyrex tubing, Knudsen limiting law behavior, $P_1/P_2 = (T_1/T_2)^{1/2}$, was restored (ref. 10). Leaching refers to the dissolving action of HCl on the inner surface of the Pyrex tubing, leaving a rough, porous surface layer. Not only should nearly complete diffuse reflection be insured by such surface roughness, but also virtually complete thermal accommodation, since each gas molecule can make many collisions within the porous layer before returning to the gas phase. Figure 10 shows that as $F_C \rightarrow 1.0$, $Q_{12} \rightarrow Q_{21}$, and $a_T \rightarrow 1.000$.

On the other hand, the presence of preadsorbed layers of Argon, Krypton, and Xenon on smooth Pyrex tubes had no effect on a_E for helium (ref. 11). In terms of the simple model, no detailed explanation can be offered now. Note that although the molecular weights of these preadsorbed gas layers are similar to those of many metals, the layers apparently behave like Pyrex surfaces instead of metal surfaces, in the thermal transpiration effect.

Effect of Tube Dimensions

Another parameter found experimentally to affect TTR deviations is the tube length

to radius ratio. Edmonds and Hobson suggest that equation (1) is more closely approached in tubes as the tube diameter is reduced (ref. 9) or as L/r is increased. For helium in a Pyrex tube of $L/r \approx 429$, a value of $a_E = (P_1/P_2)/R_m = (0.530/0.512) \approx 1.035$ was found, substantially less than values for lower L/r tubes (ref. 9). However, it was also found that $a_E \approx 1.00$ when L/r is decreased to zero, or, when the tube becomes an aperture. Using the model presented herein with $L/r = 6.0$ yields $a_T = 1.010$, indicating that such a tube is aperture-like (case 9, table III). If $L/r = 20.0$, then $a_T = 1.112$, essentially unchanged from the value of $a_T = 1.119$ for $L/r = 14.0$, although both Q_{12} and Q_{21} were significantly reduced going to the higher L/r (case 10, table III). Unfortunately, because of excessive computer time, we were not able to investigate some of the capillaries of high L/r , say, 50 or 100 or more, used by Hobson and his co-workers.

However, the effect of such long tubes in the model can be estimated after first discussing short, aperture-like tubes. To obtain the TTR deviations in the model, it is important to have as many hot gas - cold wall and cold gas - hot wall collisions as possible; that is, trajectories of the type illustrated in figure 13(a), as opposed to those illustrated in figure 13(b). Trajectories that do not lead to a difference in transmission probabilities (especially those in the first sketch of fig. 13(b)) could be expected to predominate in tubes of small L/r , causing them to act as apertures in the thermal transpiration effect.

In very long tubes, not as many incoming gas molecules reach the vicinity of the wall-temperature change in the middle of the tube, even though the percentage of diffuse

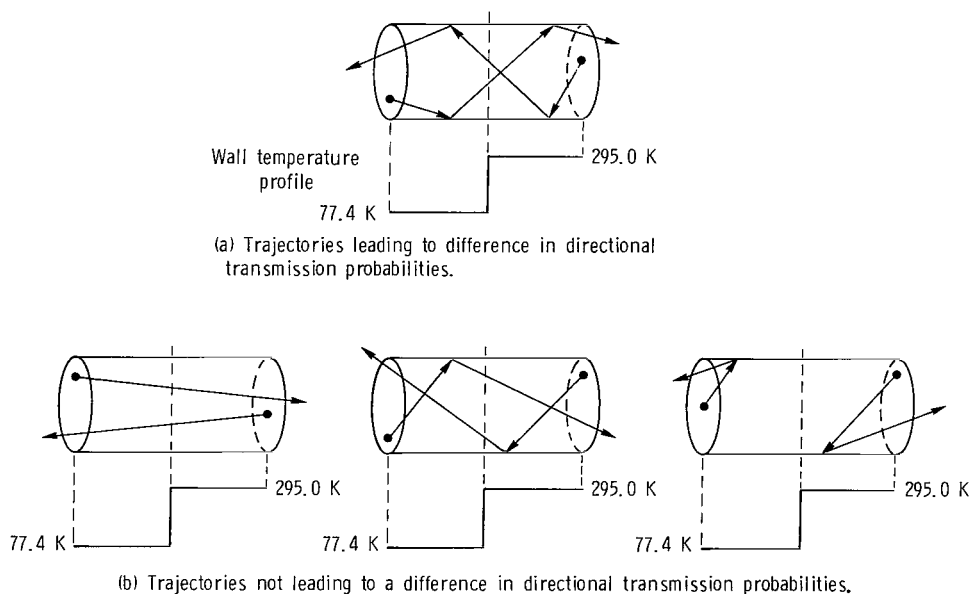


Figure 13. - Sample molecular trajectories in tubes with step function wall temperature profiles shown.

reflections is only 30 percent, as is assumed in most of the present calculations. In a very long tube, the number of diffuse reflections increases, which has the effect of erasing molecules' past history. So, even though hot-gas molecules are aided slightly near the middle of the tube and cold molecules are slightly hindered there, the L/r can be so large that the net separation effect on molecules successfully traversing the entire tube is lost, resulting in $Q_{12} \cong Q_{21}$. Hence, we believe the model would predict that $a_T \rightarrow 1.00$ as $L/r \rightarrow \infty$, assuming the wall-temperature discontinuity is near the middle of the tube.

Effect of Incoming Hot Gas - Hot Tube Section Temperature

The model indicates that the gas-surface temperature ratio is important in determining the observed TTR deviations. To our knowledge, a thorough experimental study of the effect of varying gas and surface temperatures from the conveniently obtainable liquid nitrogen and room temperatures has not been made. In the model, T_2 was changed from 295.0 to 600 K, resulting in a change in a_T from 1.119 to 1.162 (cases 1 and 2, table III). This trend is the same as indicated in Hobsons' three-stage accommodation pump results using $T_2 = 600$ K instead of 295.0 K (ref. 11). As previously stated, our single-tube results cannot reliably be extrapolated to predict pump ratios across a three-stage pump because of uncontrolled and unpredictable variations in surface conditions (ref. 11), and possible nonMaxwellian tube entry conditions in such a pump.

Predicted Axial Variation of Gas Temperature

The technique for calculating transmission probabilities readily allows calculation of the average temperature of incident gas molecules at any axial position, as well as the average temperatures of the molecules leaving the tube through the two end planes. It is important to note again that we are ascribing to each gas molecule the property of temperature, regarding temperature as a measure of average gas molecular kinetic energy. Hence, the following results should be regarded only as first-order indications of how gas temperature would vary axially, with partial LKS lobular scattering and low temperature accommodation at the tube wall.

Shown in figure 14 are the average temperatures of gas molecules striking the tube wall as functions of axial position. The temperatures are calculated for 10 000 molecules entering the cold end (fig. 14(a)) and then for 10 000 molecules entering the hot end (fig. 14(b)), with $F_C = 0.3$ and $\alpha = 0.35$. Then, these calculations were repeated with

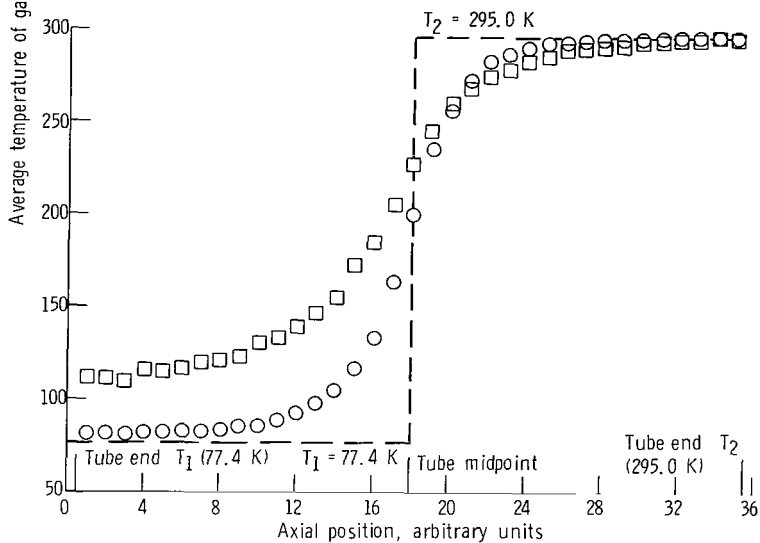
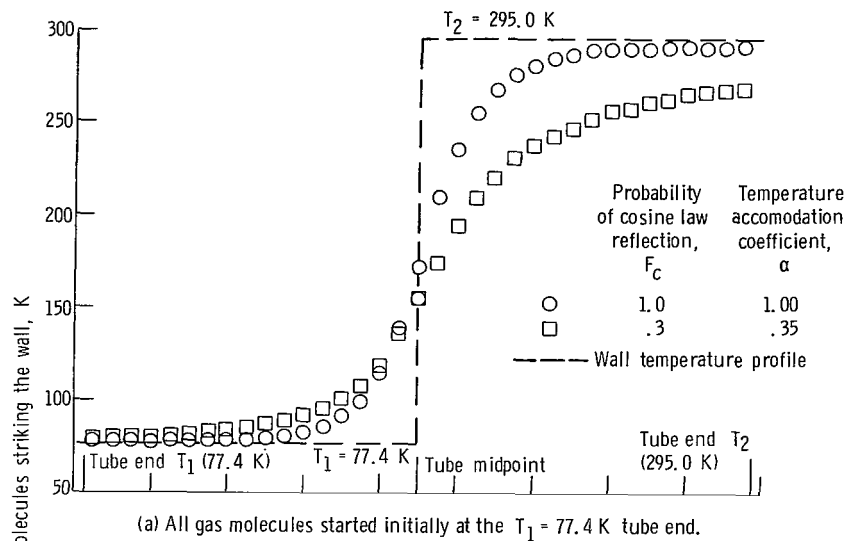


Figure 14. - Average temperature of gas molecules striking the tube wall as function of axial position. Tube length to radius ratio, 14.0; number of Monte Carlo trials, 10 000 (in each direction); gas to surface atomic mass number ratio, 0.21; wall temperature step function at $L/2$ between T_1 and T_2 tube sections.

$F_C = 1.0$ and $\alpha = 1.0$. When $F_C = 0.3$ and $\alpha = 0.35$, the originally hot gas has only cooled down to about 110 K when it strikes the walls near the cold end (fig. 14(b)), and the originally cold gas has only heated up to about 270 K near the walls of the hot end (fig. 14(a)).

The average temperatures of molecules leaving both tube ends, summarized in table V, reveal even more discrepancy between gas and wall temperature: When

TABLE V. - COMPARISON OF CALCULATED AVERAGE TEMPERATURES OF GAS
MOLECULES LEAVING TUBE THROUGH EXIT AND ENTRANCE PLANES

[Tube length to radius ratio, 14.0; assumed helium to Pyrex atomic mass ratio,
0.21; number of Monte Carlo trials at each end, 10 000.]

Condi- tion	Assumed probability of cosine law reflection, F_C	Assumed temperature accommodation coefficient, α	Molecules entering at tube end (a)	Calculated average temperature of molecules leaving through exit plane, T_{EX} , K	Calculated average temperature of molecules leaving through entrance plane, T_{EN} , K
1	1.0	1.00	T_1	273.8	78.8
2	1.0	1.00	T_2	96.9	293.7
3	0.3	0.35	T_1	248.2	87.6
4	.3	.35	T_2	141.3	289.1

^a $T_1 = 77.4$ K; $T_2 = 295.0$ K.

$F_C = 0.3$ and $\alpha = 0.35$, the average temperature of the originally hot gas which eventually exits the cold end is about 143.8 K, while the average temperature of the originally cold gas which eventually exits the hot end is about 246.4 K. Even when $F_C = 1.0$ and $\alpha = 1.0$, these exit temperatures are 96.9 and 273.8 K, respectively.

This difference between the gas and the wall temperature could be important when trying to assess the behavior of the gas in the chambers (bulb or elbow) at the tube ends.

Effects Peculiar to Non-Two-Bulb Data

The model we have discussed assumes that the gases in the reservoirs or the tube ends are Maxwellian. This assumption yields the cosine distribution at the entry planes and the $P_i / \sqrt{2\pi m_g k T_i}$ entry rate, which leads to equation (2). When the reservoirs are large bulbs, one would expect the Maxwellian assumption to be valid. However, if the reservoir is an elbow-shaped, ill-defined tubular region, the gas entering the tube of concern could take on a nonMaxwellian character. This may be the origin of the behavior peculiar to elbow apparatus in Hobson's experiments: larger values of a_E (in the approximate range 1.08 to 1.31 for helium in Pyrex tubing) and a sensitivity of a_E to liquid-nitrogen height up the tube.

If an elbow-like reservoir is assumed, it is not at all certain the the directions of the molecules on the entrance plane are described by a cosine distribution. Because of a lack of detailed information about the geometric shape and surface properties of the elbow joint beyond the entrance plane, it is difficult to estimate the directions of entering molecules. Dayton points out that in calculating tube conductances, one must consider the beaming pattern across the entrance as well as the temperature and back-scattering characteristics of surfaces beyond the exit of the tube (ref. 50). It is well known that unlike the cosine efflux pattern from a small hole in a bulb reservoir, tubes even with an L/r as small as 2.0 exert a considerable beaming effect in an axial direction on exiting molecules, as shown, for example, by Chubb (ref. 51). The only work on rarefied flow through elbows (by Davis, ref. 16) deals only with transmission probabilities, not efflux patterns, but one could reasonably expect some type of beaming effect here too.

In the present model, the use of two different entry distributions designed to beam incoming molecules down the tube more axially than a cosine distribution on the entrance plane did not result in the larger values of a_T suggested by elbow experiments.

Another theoretical difficulty inherent in the elbow reservoir is that it may not allow enough gas-surface interactions to insure that the gas temperature equals the wall temperature. Results in the previous section indicate that the gas temperature can be substantially different from the wall temperature near the tube ends, for gases with small accommodation coefficients and for a tube L/r of 14.0. Consequently, incorrectly assumed temperatures in equation (2), as well as a difference in Q_{12} and Q_{21} , help determine the behavior of the deviations of P_1/P_2 from the Knudsen limiting law (eq. (1)) observed in the elbow data.

At present, however, not enough is known about nonMaxwellian entry conditions to warrant detailed modifications of the current model, in an attempt to explain the elbow TTR effects.

Comments on Accommodation Pumping

The action of the accommodation pump of Hobson (fig. 6(c)) can be qualitatively explained by considering transmission probabilities in the present model. Note that the pump is constructed of alternating smooth and rough (leached) sections of Pyrex tubing. Our calculations show that the transmission probabilities of molecules moving in the hot (top) to cold (bottom) direction in the smooth tube sections are greater than those found for molecules moving in the cold-to-hot direction because of temperature-dependent lobular scattering. On the other hand, the rough, leached tube sections, probably having an $F_C \cong 1.0$, would not be expected to sustain much lobular scattering, and thus, in

these sections, transmission probabilities in the hot-to-cold direction would nearly equal those in the cold-to-hot direction. Thus, in effect, each adjacent pair of smooth and rough tubes will, because of the differential transmission probabilities, act as a pump. In the accommodation pump, each such stage acts in series with other stages to multiply the overall pumping effect.

SUMMARY OF RESULTS

A model of free molecular gas flow in tubes was developed that combines a lobular reflection distribution with conventional cosine law (diffuse) reflection at the wall using a Monte Carlo approach to the solution. At each gas-wall collision, an incoming molecule is either reflected diffusively with probability F_C , or it is reflected in a direction chosen from the Logan-Keck-Stickney lobular reflection distribution, with probability $1 - F_C$. Assumed temperature accommodation coefficients determine the temperature, or average kinetic energy, of the gas molecule after the interaction, in either case. This lobular distribution is a function of incident gas and surface temperatures, incidence angle, and gas-to-surface atomic mass ratio and has successfully predicted a number of observed gas molecular-beam surface-scattering patterns.

The model was used to explain previously observed deviations in the free molecular thermal transpiration ratio from the Knudsen limiting law. These deviations suggest that when two reservoirs at temperatures T_1 and T_2 are joined by glass tubing, gas molecules are more likely to traverse the tube in the hot-to-cold direction than in the cold-to-hot direction; that is, $Q_{21} > Q_{12}$ when $T_2 > T_1$, where Q_{ij} is the tube transmission probability from reservoir i to reservoir j .

The major results from the calculation of Q_{12} and Q_{21} using the model are the following:

1. Theoretically calculated values of $a_T = Q_{21}/Q_{12}$ are in the range 1.09 to 1.14 for helium when F_C is assumed to be 0.3 (the same for all gas-wall collisions), when $T_1 = 77.4$ K and $T_2 = 295.0$ K, and when the tube $L/r = 14.0$. This is consistent with some previous thermal transpiration ratio data obtained with Pyrex tubing joining two glass bulb reservoirs (two-bulb data).

2. When part of the length of the tube is assumed to be at T_1 and the remainder at T_2 , the average number of gas-wall collisions per incoming gas molecule is greater in the $T_1 \rightarrow T_2$ direction than in the $T_2 \rightarrow T_1$ direction. The difference arises from collisions after the molecules across the wall-temperature break, which was placed near the tube's center to approximate experimental conditions. This means that initially hot molecules make slightly fewer wall collisions, on the average, than initially cold molecules starting from the opposite tube end.

3. Values of a_T are relatively insensitive to changes in the wall-temperature distribution between the T_1 and T_2 tube ends. Also, $a_T > 1.00$ even when the entire tube is at T_1 or T_2 . Both findings agree with previous two-bulb data.

4. Values of a_T are fairly insensitive to varying the thermal accommodation coefficients between 0.35 and 1.00.

5. The model confirms the following experimental trends: The transmission probability ratio a_T

- (a) decreases to 1.00 as the tube length-to-radius ratio approaches that of an aperture, zero
- (b) decreases toward 1.00 as the tube wall becomes microscopically rougher (assuming F_C increases as roughness increases)
- (c) increases as the hot gas - hot tube section temperature increases
- (d) decreases as gas molecular mass increases (by changing the gas-to-surface mass ratio; but, more reasonably, by assuming F_C increases as m_g increases).

6. The model is qualitatively consistent with Hobson's accommodation pump studies, which used such tubes with transmission probability directional differences.

Lewis Research Center,
National Aeronautics and Space Administration,
Cleveland, Ohio, November 19, 1971,
113-31.

APPENDIX - SYMBOLS

A_1, A_2	tube entrance planes
a_E	experimental thermal transpiration ratio, (temperature normalized), $(P_1/P_2)/R_m$
a_T	transmission probability ratio, Q_{21}/Q_{12}
B_1, B_2	quantities in LKS equation (eq. (3))
$\cos(A_1), \cos(B_1), \cos(C_1)$	direction cosines of particle trajectories, with x, y, z axes, respectively
F_C	probability of cosine law (diffuse) reflection
F_L	probability of lobular reflection, $1 - F_C$
$f(u)$	probability density function
$K_{GW}(i, j)$	average number of gas-wall collisions per incoming gas molecule at T_i , moving generally in the T_j direction; $i, j = 1, 2$
K_O	number of Monte Carlo trials
k	Boltzmann constant, $1.38054 \times 10^{-23} \text{ JK}^{-1}$
L	tube length, m
LKS	Logan-Keck-Stickney
m_g	gas atomic mass number
m_s	surface atomic mass number
P_A, P_B	pressures at end of an accommodation pump
P_i	gas pressure in region i ; $i = 1, 2$
$P_N(\theta_r)$	$P(\theta_r)/P(\theta_{\max})$
$P(\theta_r)$	probability of reflection into $d\theta_r$ at θ_r , given by LKS equation (eq. (3))
p	probability of falsity of inequality in eq. (10b)
Q_D	direct tube transmission probability
Q_{ij}	tube transmission probability in $i \rightarrow j$ direction; $i, j = 1, 2$
R	thermal transpiration ratio (P_1/P_2)
R_i	random variable uniformly distributed on the interval (0,1)

R_m	$(T_1/T_2)^{1/2}$
r	tube radius, m
$\{S_i\}$	set of random numbers
T_{EN}	average temperature of gas molecules leaving tube through entrance plane, K
T_{EX}	average temperature of gas molecules leaving tube through exit plane, K
T_g	gas temperature, K
T_i	gas temperature in region i , K; $i = 1, 2$
T_{OUT}, T_{IN}	temperature of gas molecules leaving and approaching tube wall, respectively, K
T_R	surface-to-gas temperature ratio, T_s/T_g
T_s	surface temperature, K
$T_s(z)$	wall-temperature distribution as function of axial coordinate z , K
TTR	thermal transpiration ratio
u	variable in probability density function
u_0, u_1	limiting values of u
x_i, y_i, z_i	coordinates of particle position in tube model
α	temperature accommodation coefficient
α_C	temperature accommodation coefficient for cosine reflections
α_L	temperature accommodation coefficient for lobular reflections
ϵ_C	Chevyshev confidence limit
ϵ_N	95-percent confidence limit for Q_{ij} assuming normal distribution of Monte Carlo answers
η	random variable
θ_i	angle of incidence, measured from surface normal, deg
θ_{max}	value of θ_r at which $P(\theta_r)$ is maximum
θ_r	angle of reflection, measured from surface normal, deg
θ_{spec}	specular reflection direction, $= \theta_i$, deg

$\Delta\theta$	$\theta_{\max} - \theta_{\text{spec}}$
μ	m_g/m_s
ξ	random variable

REFERENCES

1. Reynolds, O.: On Certain Dimensional Properties of Matter in the Gaseous State. Phil. Trans. Roy. Soc. London, vol. 170, 1879, pp. 727-848.
2. Knudsen, Martin: A Revision of the Equilibrium Condition of Gases. Thermal Molecular Flow. Ann. Phys., vol. 31, 1910, pp. 205-229.
3. Knudsen, Martin: Thermal Molecular Flow of Gases Through Tubes and Porous Bodies. Ann. Phys., vol. 31, 1910, pp. 633-640.
4. Weber, S.; and Schmidt, G.: Experiments on the Thermo-Molecular Pressure Difference in the Region of the Boundary Condition $P_1/P_2 = \sqrt{T_1/T_2}$. K. Onnes Lab., Leiden, Comm. No. 246C, 1938.
5. Bennett, M. J.; and Tompkins, F. C.: Thermal Transpiration: Application of Laing's Equation. Trans. Faraday Soc., vol. 53, 1957, pp. 185-192.
6. Rosenberg, A. J.; and Martel, C. S., Jr.: Thermal Transpiration of Gases at Low Pressures. J. Phys. Chem., vol. 62, no. 4, Apr. 1958, pp. 457-459.
7. Podgurski, H. H.; and Davis, F. N.: Thermal Transpiration at Low Pressure. The Vapor Pressure of Xenon Below 90° K. J. Phys. Chem., vol. 65, no. 8, Aug. 1961, pp. 1343-1348.
8. Hobson, J. P.; Edmonds, T.; and Verreault, R.: Thermal Transpiration in Helium in the Pressure Range 10^{-8} to 20 Torr. Can. J. Phys., vol. 41, no. 6, June 1963, pp. 983-985.
9. Edmonds, T.; and Hobson, J. P.: A Study of Thermal Transpiration Using Ultrahigh-Vacuum Techniques. J. Vac. Sci. Tech., vol. 2, no. 4, July-Aug. 1965, pp. 182-197.
10. Hobson, J. P.: Surface Smoothness in Thermal Transpiration at Very Low Pressures. J. Vac. Sci. Tech., vol. 6, no. 1, Jan.-Feb. 1969, pp. 257-259.
11. Hobson, J. P.: Accommodation Pumping - A New Principle for Low Pressures. J. Vac. Sci. Tech., vol. 7, no. 2, Mar.-Apr. 1970, pp. 351-357.
12. Miller, George A.; and Buice, Ralph L., Jr.: On the Knudsen Limiting Law of Thermal Transpiration. J. Phys. Chem., vol. 70, no. 12, Dec. 1966, pp. 3874-3880.
13. Maxwell, J. C.: Collected Works. Vol. 2, 1879, pp. 707-708.
14. Hobson, J. P.: Analysis of Accommodation Pumps. J. Vac. Sci. Tech., vol. 8, no. 1, Jan.-Feb. 1971, pp. 290-293.

15. Fan, Chien: Monte Carlo Solution of Mass, Momentum and Energy Transfer for Free Molecule and Near Free Molecule Flow through Circular Tubes. Rep. LMSC/HREC-A791015, Lockheed Missiles and Space Co., Dec. 1967.
16. Davis, D. H.: Monte Carlo Calculation of Molecular Flow Rates through a Cylindrical Elbow and Pipes of Other Shapes. *J. App. Phys.*, vol. 31, no. 7, July 1960, pp. 1169-1176.
17. Smith, Craig G.; and Lewin, Gerhard: Free Molecular Conductance of a Cylindrical Tube with Wall Sorption. *J. Vac. Sci. Tech.*, vol. 3, no. 3, May-June 1966, pp. 92-95.
18. Chubb, J. N.: Monte Carlo Analysis of Pumping Speed Test Dome Performance for Several Vapour Diffusion Pump Geometries. *Vacuum*, vol. 16, no. 11, 1966, pp. 591-596.
19. Chubb, J. N.: Performance Assessment of Condensation Pumping. *Vacuum*, vol. 16, no. 12, 1966, pp. 681-689.
20. Brown, R. F.; Powell, H. M.; and Trayer, D. M.: Studies of the Velocity Distributions of Incident and Reflected A Beams. *Rarefied Gas Dynamics. Vol. 2.* Leon Trilling and Harold Y. Wachman, eds., Academic Press, 1969, pp. 1187-1190.
21. Fisher, S. S.; Hagen, O. F.; and Wilmoth, R. G.: Flux and Speed Distributions of Molecular Beams after Scattering by Metal Surfaces. *J. Chem. Phys.*, vol. 49, no. 4, Aug. 15, 1968, pp. 1562-1571.
22. Ballance, James O.: The Molecular Kinetics of the Bayard-Alpert and Modified Redhead Vacuum Gauges Used on Explorer XVII and Explorer XXXII. NASA TM X-53838, 1969.
23. Logan, R. M.; Keck, J. C.; and Stickney, R. E.: Simple Classical Model for the Scattering of Gas Atoms from a Solid Surface: Additional Analyses and Comparisons. *Rarefied Gas Dynamics. Vol. 1.* C. L. Brundin, ed., Academic Press, 1967, pp. 49-66.
24. Stickney, Robert E.: Atomic and Molecular Scattering from Solid Surfaces. *Advances in Atomic and Molecular Physics. Vol. 3.* D. R. Bates and Immanuel Estermann, eds., Academic Press, 1967, pp. 143-204.
25. Stickney, R. E.; Logan, R. M.; Yamamoto, S.; and Keck, J. C.: Simple Classical Model for the Scattering of Gas Atoms from a Solid Surface: III. Analyses for Monoenergetic Beams and Lock-in Detector Signals. *Fundamentals of Gas-Surface Interactions.* Howard Saltsburg, J. N. Smith, Jr., and Milton Rogers, eds., Academic Press, 1967, pp. 422-434.

26. Smith, Joe N., Jr.; Saltsburg, Howard; and Palmer, Robert L.: Scattering of Velocity-Filtered Atomic Beams of Ar and Xe from the (111) Plane of Silver. *J. Chem. Phys.*, vol. 49, no. 3, Aug. 1, 1968, pp. 1287-1297.
27. Hinchey, John J.; and Foley, William M.: Scattering of Molecular Beams by Metallic Surfaces. *Rarefied Gas Dynamics*. Vol. 2. J. H. deLeeuw, ed., Academic Press, 1966, pp. 505-517.
28. Logan, R. M.; and Stickney, R. E.: Simple Classical Model for the Scattering of Gas Atoms from a Solid Surface. *J. Chem. Phys.*, vol. 44, no. 1, Jan. 1, 1966, pp. 195-201.
29. O'Keefe, D. R.; and Palmer, R. L.: Atomic and Molecular Beam Scattering from Macroscopically Rough Surfaces. *J. Vac. Sci. Tech.*, vol. 8, no. 1, Jan.-Feb. 1971, pp. 27-30.
30. Hurlbut, F. C.: Molecular Scattering at the Solid Surface. *Recent Research in Molecular Beams*. Immanuel Estermann, ed., Academic Press, 1959, pp. 145-156.
31. Logan, R. M.; and Keck, James C.: Classical Theory for the Interaction of Gas Atoms with Solid Surfaces. *J. Chem. Phys.*, vol. 49, no. 2, July 15, 1968, pp. 860-876.
32. Logan, R. M.: Calculation of the Energy Accommodation Coefficient Using the Soft - Cube Model. *Surface Sci.*, vol. 15, 1969, pp. 387-402.
33. Goodman, Frank O.: Quantum Mechanical Basis for the Cubes Models in Gas-Surface Scattering Theory, and an Experimental Test. *J. Chem. Phys.*, vol. 53, no. 6, Sept. 15, 1970, pp. 2281-2283.
34. Trilling, Leon: Theory of Gas-Surface Collisions. *Fundamentals of Gas-Surface Interactions*. Howard Saltsburg, J. N. Smith, Jr., and Milton Rogers, eds., Academic Press, 1967, pp. 392-421.
35. Shreider, Yu. A., ed.: *The Monte Carlo Method*. Pergamon Press, 1966.
36. Knudsen, Martin H. C.: *The Kinetic Theory of Gases*. Third ed., John Wiley & Sons, Inc., 1950.
37. Hinchey, John J.; Malloy, Evelyn S.; and Carroll, James B.: Scattering of Thermal Energy Gas Beams by Metallic Surfaces II. Rep. F-910439-7, United Aircraft Research Labs. June 1967. (Available from DDC as AD-653720.)
38. Jakus, Karl: Experimental Investigation of Gas-Surface Re-emission Distributions Using Continuum Source Molecular Beam Techniques. Rep. AS-68-7, California University, Berkeley, Sept. 1968.

39. Schäfer, Kl.; and Gerstacker, H.: Adsorption, partielle thermische Akkommodation von Gasen an Oberflächen und ihr Zusammenhang mit katalytischen Wirkungen. *Zeit. f. Elektrochemie*, vol. 60, no. 8, 1956, pp. 874-887.
40. Goodman, Frank O.: Interaction Potentials of Gas Atoms with Cubic Lattices on the 6-12 Pairwise Model. *Phys. Rev.*, vol. 164, no. 3, Dec. 15, 1967, pp. 1113-1123.
41. Richley, Edward A.; and Reynolds, Thaine W.: Numerical Solutions of Free-Molecule Flow in Converging and Diverging Tubes and Slots. NASA TN D-2330, 1964.
42. DeMarcus, W. C.: The Problem of Knudsen Flow. Part III. Solutions for One-Dimensional Systems. Rep. K-1302, Part III, Oak Ridge Gaseous Diffusion Plant, Mar. 19, 1957.
43. Clausing, P.: The Flow of Very Rarefied Gases Through Tubes of Any Length. *Ann. Phys.*, vol. 12, no. 8, Mar. 1932, pp. 961-989.
44. Ward, John W.; and Fraser, Malcolm V.: Study of Some of the Parameters Affecting Knudsen Effusion. VI. Monte Carlo Analyses of Channel Orifices. *J. Chem. Phys.*, vol. 50, no. 4, Feb. 15, 1969, pp. 1877-1882.
45. Miller, A. R.: The Fraction of Effusing Molecules Striking a Collector Plate over a Circular Capillary. Rep. AN-1328, Aerojet-General Nucleonics, Dec. 1964. (Available from DDC as AD-454732.)
46. Helmer, John C.: Solution of Clausing's Integral Equation for Molecular Flow. *J. Vac. Sci. Tech.*, vol. 4, no. 6, Nov.-Dec. 1967, pp. 360-363.
47. DeMarcus, W. C.: The Problem of Knudsen Flow. Part IV. Specular Reflection. Rep. K-1302, Part IV, Oak Ridge Gaseous Diffusion Plant, Mar. 27, 1957.
48. Lund, L. M.; and Berman, A. S.: Flow and Self-Diffusion of Gases in Capillaries. Part II. *J. Appl. Phys.*, vol. 37, no. 6, May 1966, pp. 2496-2508.
49. Thomas, Lloyd B.: Thermal Accommodation of Gases on Solids. *Fundamentals of Gas-Surface Interactions*. Howard Saltsburg, J. N. Smith, Jr., and Milton Rogers, eds., Academic Press, 1967, pp. 346-369.
50. Dayton, B. B.: The Measured Speed of an "Ideal Pump." *Vacuum*, vol. 15, no. 2, Feb. 1965, pp. 53-57.
51. Chubb, J. N.: A Monte Carlo Computer Program for Analysis of Molecular Gas Flow. Rep. CLM-R-54, Culham Laboratory, United Kingdom Atomic Energy Authority, Dec. 1965.

NATIONAL AERONAUTICS AND SPACE ADMINISTRATION
WASHINGTON, D.C. 20546

OFFICIAL BUSINESS
PENALTY FOR PRIVATE USE \$300

FIRST CLASS MAIL

POSTAGE AND FEES PAID
NATIONAL AERONAUTICS AND
SPACE ADMINISTRATION



018 001 C1 U 06 720204 S00903DS
DEPT OF THE AIR FORCE
AF WEAPONS LAB (AFSC)
TECH LIBRARY/WLOL/
ATTN: E LOU BOWMAN, CHIEF
KIRTLAND AFB NM 87117

POSTMASTER: If Undeliverable (Section 158
Postal Manual) Do Not Return

"The aeronautical and space activities of the United States shall be conducted so as to contribute . . . to the expansion of human knowledge of phenomena in the atmosphere and space. The Administration shall provide for the widest practicable and appropriate dissemination of information concerning its activities and the results thereof."

— NATIONAL AERONAUTICS AND SPACE ACT OF 1958

NASA SCIENTIFIC AND TECHNICAL PUBLICATIONS

TECHNICAL REPORTS: Scientific and technical information considered important, complete, and a lasting contribution to existing knowledge.

TECHNICAL NOTES: Information less broad in scope but nevertheless of importance as a contribution to existing knowledge.

TECHNICAL MEMORANDUMS: Information receiving limited distribution because of preliminary data, security classification, or other reasons.

CONTRACTOR REPORTS: Scientific and technical information generated under a NASA contract or grant and considered an important contribution to existing knowledge.

TECHNICAL TRANSLATIONS: Information published in a foreign language considered to merit NASA distribution in English.

SPECIAL PUBLICATIONS: Information derived from or of value to NASA activities. Publications include conference proceedings, monographs, data compilations, handbooks, sourcebooks, and special bibliographies.

TECHNOLOGY UTILIZATION PUBLICATIONS: Information on technology used by NASA that may be of particular interest in commercial and other non-aerospace applications. Publications include Tech Briefs, Technology Utilization Reports and Technology Surveys.

Details on the availability of these publications may be obtained from:

**SCIENTIFIC AND TECHNICAL INFORMATION OFFICE
NATIONAL AERONAUTICS AND SPACE ADMINISTRATION
Washington, D.C. 20546**